Antibacterial activities of *Macrotermes bellicosus* metabolite-mediated silver nanoparticles against isolates from patients with diabetic foot infection

By

SHAIBU, Bose Ozohu
(M.Tech/SLS/2017/6829)

DEPARTMENT OF MICROBIOLOGY
FEDERAL UNIVERSITY OF TECHNOLOGY,
MINNA

SEPTEMBER, 2021

ANTIBACTERIAL ACTIVITIES OF CRUDE *Macrotermes bellicosus* EXTRACT-MEDIATED SILVER NANOPARTICLES AGAINST ISOLATES FROM DIABETIC PATIENTS WITH FOOT INFECTION

By

SHAIBU, Bose Ozohu
(M.Tech/SLS/2017/6829)

A THESIS SUBMITTED TO THE POSTGRADUATE SCHOOL, FEDERAL UNIVERSITY OF TECHNOLOGY, MINNA, NIGERIA IN PARTIAL FULFILMENT OF THE REQUIREMENTS FOR THE AWARD OF THE DEGREE OF MASTERS OF TECHNOLOGY (M. Tech) IN PHARMACEUTICAL MICROBIOLOGY

SEPTEMBER, 2021

ABSTRACT

Diabetic foot infections (DFI) are commonly refered to a breech in the skin epithelium involving the distal to the ankle joints in a person suffering from diabetes mellitus.The antibacterial activity of crude extract and extract mediated silver nanoparticles of *Macrotermes bellicosus* (Soldier termites) were investigated against isolates from patients with diabetic foot infection using agar diffusion method. Extraction of powdered insect gave rise to crude ethanol extract, n-hexane (Eh), ethylacetate (Eoac) and (Ee), aqueous (Eaq) fractions. Cyanides, saponins, phytates, phenols, flavonoids, alkaloids, tannins and proteins were detected in the crude extract and fractions. Treatment of extract and fractions with silver nitrate (2mM) produced a dark-brown spherical and aggregated shaped nanoparticles with absorbance peaks from lowest to highest nm (390, 395, 400 and 410 nm). The Eaoc-AgNPs at 200mg/ml produced zones of inhibition of 16.00 ±1.00, 6.47 ± 0.58 and 30.67 ± 2.08 mm against *P.aeruginosa*, *S. pyogenes* and *K. pneumoniae* respectively. The MIC of Eoac-AgNPs for *P.aeruginosa, S. pyogenes* and *K. pneumoniae* was at 6.25, 1.25 and 25.0 mg/ml respectively while the MBC was at 12.5, 50.0 and 6.25 mg/ml. The Eoac-AgNPs was bacteriocidal on the test isolates. There was significant ($P \leq 0.05$) wound closure observed in rats (groups 1-6) treated with Eoac-AgNPs from day 0 (1.23± 0.12-1.27±0.30 mm) to day 14 (0.67±0.25-0.33±0.10 mm) compared to group 7 (diabetes + wound only) at 1.13±0.21 mm. Treatment of rats with ointment showed wound healing characterized by the presence of collagen, granulation tissues, few inflammatory cells and complete epitelialization. The application of Eoac-AgNPs ointment on the rats did not produce allergic reactions, dermatitis or death. These findings showed that *M.bellicosus* could be useful in treating infected ulcer.

TABLES OF CONTENTS

LIST OF TABLES

LIST OF FIGURES

LIST OF PLATES

LIST OF ABBREVIATIONS

Abbreviation	Meaning
-	Negative
%	Percentage
+	Positive

°C	Degree celsius
α	Alpha
$AgNO_3$	Silver nitrate
ANOVA	Analysis of variance
BA	Blood agar
CAT	Catalase
CIT	Citrate
CLSI	Clinical and Laboratory Standard Institute
cm^3	Centimeter cube
CoA	Coagulase
DPX	Distyrene plasticizer
Eaq	Aqueous extract
Eaq-AgNPs	Aqueous extract-mediated silver nanoparticles
EDS	Energy dispersive spectrum
Ee	Extract of ethanol
Ee-AgNPs	Ethanol extract-mediated silver nanoparticles.
Eh	Extract of n-hexane
Eh-AgNPs	n-hexane extract-mediated silver nanoparticles
Eoac	Extract of ethylacetate
Eoac-AgNPs	Ethylacetate extract-mediated silver nanoparticles
ESC	Extract sterility control
F	Fructose
FTIR	Fourier transform infrared spectroscopy
G	Glucose
GR	Gram's reaction
H_2O_2	Hydrogen peroxide
H_2S	Hydrogen sulphide
H_2SO_4	Tetraoxosulphate (vi) acid
Hcl	Hydrogen chloride
IND	Indole

KOH	Pottassium hydroxide
L	Lactose
MBC	Minimum bactericidal concentration
MCA	McConkey agar
mg/dL	Milligram per deciliter
mg/kg bw	Milligram per kilogram body weight
mg/mL	Milligram per Millitre
MHA	Mueller-Hinton agar
MIC	Minimum inhibitory concentration
mL	Milliliter
mm	Millimetre
MR	Methyl red
MSC	Medium sterility control
NA	Nutrient agar
NaCl	Sodium chloride
NaOH	Sodium hydroxide
NB	Nutrient broth
ND	Not detected
NIPRD	National Institute for Pharmaceutical Research Development
nm	Nanometer
OVC	Organism viability count
OX	Oxidase
S	Sucrose
SEM	Scanning electron microscopy
SPSS	Statistical package for social sciences
TSI	Triple sugar iron
USA	United States of America
UV	Ultra Violet
VP	Vogues proskauer
WC	Wound control

XRD	X-ray diffraction
ZOI	Zones of inhibition
β	Beta
γ	Gamma

LIST OF APPENDICES

LIST OF EQUATIONS

CHAPTER ONE

1.0 INTRODUCTION

1.1 Background to the Study

Diabetes mellitus (DM) is a multiple group of metabolic disorders that is often accompanied with elevated disease burden in developing countries such as Nigeria. Diabetes clearly has transformed the geomorphology of health care especially in Nigeria and West Africa over the decades which has been linked to the resurgence of tuberculosis and with the rising frequency of end-stage kidney disease, erectile dysfunction, and stroke (Arman *et al*., 2020). Diabetes has also led to elevated numbers in the bulk of cases of lower extremity amputation (LEA) in Nigeria. Patients with diabetes have prolonged Hospital stay and highest medical bills on medical wards with diverse complications, such as high blood pressure, stroke, heart failure and fetid foot gangrene (Skyler *et al*., 2017). Diabetes mellitus remains one of the most exorbitant diseases to control largely which is due to associated complications and the chronicity. It is observed that diabetes is prevalent in a quarter to a third of all hospital admissions in Nigerian medical (nonsurgical) wards and it is also one of the leading

predisposing factors to operative obstetric delivery, premature births, neonatal mortality and reduced quality of life (Aguocha *et al*., 2018). Diabetic foot infections (DFI) are commonly refered to a breech in the skin epithelium involving the distal to the ankle joints in a person suffering from diabetes mellitus. Up to 20% of diabetes-related hospital admission worldwide and 2.2million mortality were ascribable to elevated blood glucose level and diabetic foot ulcers in 2012 (WHO, 2020).

Nigeria has witnessed more than 100 % increase in the prevalence of the disease, from 2.2% in 1997 to nearly 8% in 2020 in the last two decades (World Health Organization, 2020).

The most significant bacteria in diabetic foot infections are *Escherichia coli*, *Staphylococcus aureus* which is the most common pathogen with *Streptococcus* spp, *Klebsiella pneumoniae Enterococcus*, *Enterobacteriaceae* and *Pseudomonas aeruginosa* (Raimi and Fasanmade, 2018). Risk factors for developing diabetic foot ulcers are manageable, but poor outcomes of foot complications may be due to poor awareness among patients and some cadre of health care personnels, poor and delayed access to health care, poor referrals for specialist treatment, lack of team approach for the treatment of the complicated diabetic foot, absence of refresher training programmes for health care providers and lack of quality assuarance programme (Raghav *et al*., 2018).

For the successful treatment of DFIs, the administration of antimicrobial agents alone is insufficient without accompanying proper wound care. Nevertheless, the choice of appropriate empirical antibiotics is important to reduce treatment failure (Raimi and Fasanmade, 2018). The incidence of antimicrobial resistance and adverse effects; have led to growing interest among consumers against synthetic additives, thereby diverting the trend towards natural products. Animals have been methodologically tested by pharmaceautical

companies as sources of drugs for modern medical science and the current number of animal sources for producing essential medicines is quite impressive (Nada *et al*., 2017). The chemical constituents and pharmacological actions of some animal products are already known to some extent, and ethnopharmacological studies focused on animal medicines could be very important in clarifying the eventual therapeutic usefulness of this class of biological remedies (Suciu *et al*., 2020).

However, just like plants, insects also produce complex suites of chemicals (metabolites). Most insects produce these complex chemicals for various purposes including defense, mating, communication and other processes that help the insects to survive (Verma and Prasad, 2018). These insects' metabolites have been recognized for having potent immune defenses that produce constitutive and inducible antimicrobial compounds to combat various pathogens. Thus, they have been targeted as a potential source of antimicrobial compounds. When pathogens break through morphological barriers, insects evoke innate immune responses comprised of cellular and humoral reactions. Cellular reactions are hemocyte-mediated and include phagocytosis and encapsulation, while humoral reactions involve the production of antimcrobial proteins and activation of enzymatic cascades (Yi *et al*., 2017).

Termites are known to produce metabolites from their gut which are useful in pharmaceuticals and local medicines. Termites belong to the family of "termitidae" and order, "Isoptera". They are called 'odna' in Gbagi, 'ekar' in Nupe, 'ivo' in Ebira, 'esusu' in Yoruba, 'aku' in Ibo, and 'chinge' in Hausa. This species of termite are insects with typical colony containing nymphs (semi-mature young), workers, soldiers and the reproductive individuals (queen and king).

Macrotermes nigeriensis is locally used in Nigeria to treat wounds, sickness of pregnant women and as charm for spiritual protection. Some antibiotic compounds isolated from

termites have also been used for treating microbial infections such as sinusitis, bronchitis and skin infections (Endo *et al*., 2020). Due to longer duration of illness and treatment in hospitals, there is increase in health care costs as well as the economic burden on families and societies. The achievements of modern medicine (synthetic antibiotics) are put at risk by multi-drug resistant microorganisms commonly associated with DFIs. Since antibiotics such as synthetic and natural products are no longer as effective as before, new drugs are urgently needed.

Nano-synthesized materials are included among the new promising drugs for controlling resistant bacteria infections (Xu *et al*., 2017). Recent studies on this topic indicate that nano-materials are strong candidates for being safe and efficacious chemotherapeutic agents (Endo *et al*., 2020).Without effective antimicrobials for prevention and treatment of diabetic foot infections, the conjugation of termite gut and nanoparticles thus presents a novel habitat for searching new antibiotic producing metabolites.

1.2 Statement of the Research Problem

In addition to being the prime factor associated with amputation, diabetic foot infections account for more hospital admissions leading to increase in health care costs as well as economic burden on families and society.The classic signs of infection are erythema, oedema, heat, pain and purulent discharge which are not clear from the onset due to ischaemia and neuropathy in diabetic foot ulcers. Secondary signs of infection such as serious exudates, delayed healing, friable granulation tissue, discolored granulation tissue, foul odour, pocketing of wound base and wound breakdown are taken as evidence of infection (Min *et al*., 2016). Diabetic foot infection arises mainly from skin ulceration associated with loss of protective sensation (peripheral neuropathy), altered foot architecture and trauma. Assessing the severity of DFIs is crucial in determinig the need for hospitalization, choice of emperical

antibiotics (broad-spectrum intravenous antibiotics and narrow-spectrum oral antibiotics) (Lavery *et al*., 2017).

Diabetic foot infections in patients with diabetes are difficult to treat because these individuals have impaired microvascular circulation due to sugar-coated capillaries which limits the access of phagocytic cells to the infected area and results in poor concentration of antibiotics in the infected tissue. In addition, diabetic individuals do not only have a combined infection involving bone and soft-tisssue called fetid foot; a severe and extensive chronic soft-tissue and bone infection that causes foul exudate, but they may also have peripheral vascular disease that involve the large vessels, as well as microvascular and capillary disease that results in gangrene (Parravano *et al*., 2019). Except for chronic osteomyelitis, infections in patients with diabetes are caused by the same microorganisms that can infect the extremities of persons without diabetes. It has been estimated that the lifetime risk of a patient developing a foot ulcer is 25 % (Parravano *et al*., 2019). Application of appropriate antibiotics and the achievments of modern medicine are put at risk by multi-drug resistant microorganisms such as methicilin-resistant *Staphylococcus aureus* (MRSA) which is the most common organism with *Streptococcus, Enterococcus*,

Enterobacteriaceae, Proteus and *Pseudomonas,* making the selection of antibiotics difficult (Miyan *et al*., 2017). Therefore, there is a need to come up with cheaper, affordable and effective new bioactive treatment against isolates from diabetic foot infections.

1.3 Justification for the Study

Since the repeated use of antibiotics in the treatment of ulcerated diabetic foot are associated with increased resistant organisms such as *Escherichia coli, Pseudomonas aeruginosa,* and *Staphylococcus aureus,* there is urgent need to source from new drugs from bioactive compounds from termites' heads that are readily available, cheap and efficacious. Data

generated will add knowledge to existing information on chemotherapy of diabetic foot infection. (Jneid *et al*., 2018).

1.4 Aim and Objectives of the Study

1.4.1 Aim of the Study

To investigate the antibacterial activities of soldier Termites' metabolite-mediated silver nanoparticles against isolates from patients with diabetic foot infections.

1.4.2 Specific Objectives of the Study

i. screen crude extracts of *Macrotermes bellicosus* and extract-mediated silver nanoparticles for the presence of bioactive constituents.

ii. investigate the antibacterial potentials of crude extract of *M. bellicosus* and extractmediated silver nanoparticles on isolates from patients with diabetic foot infection. iii. determine the minimum inhibitory and minimum bactericidal concentrations of extract- mediated silver nanoparticles iv. characterize the extract-mediated silver nano particles

v. carry out topical toxicological study in rats.

CHAPTER TWO

2.0 LITERATURE REVIEW

2.1 Termites

Termites are known to produce metabolites from their gut which are useful in pharmaceuticals and local medicines. They are called ‘odna in Gbagi, ‘ekar’ in Nupe, ‘ivo’ in Ebira, ‘esusu’ in Yoruba, ‘aku’ in Igbo, and ‘chinge’ in Hausa. Since ancient times, complex interactions among humans and other animals have been recorded, including harmonic and conflicting relations (Alves *et al*., 2016). Termites illustrate this situation, as they can cause significant economic damage in urban and rural areas. At the same time, people from different parts of the world use them as food (for humans and livestock) and as a source material for popular medicine. The importance of insects as a food source for humans is not surprising, since this is the group with the highest number of species in nature, thereby representing significant biomass (Meyer-Rochow and Chakravort, 2017). Considered as important natural resources, insects are, in many ways, a basic component of the diets of humans and other animals and have played an important role as a source of medicinal resources (Chaves *et al*., 2016).

2.1.1 Description of termites and botanical classification

Termites are eusocial insects that are classified at the taxonomic rank of infraorder ‘Isoptera’, family ‘Termitidae’. Termites were once classified in a separate order from cockroaches, but recent phylogenetic studies indicate that they evolved from close ancestors of cockroaches. Division of labour exists in termites with distinct polymorphic features which

includes sterile male, female workers and soldiers (Zeng *et al*., 2016). The fertile females are called the queens while fertile males are known as kings. They feed mostly on dead plant materials and cellulose. Termite queens have the longest lifespan of any insect in the world, with some queens living up to 50 years. Unlike ants, which undergo a complete metamorphosis, each individual termite goes through an incomplete metamorphosis that proceeds through egg, nymph and adult stages (Shockley and Dossey, 2017).Termites constitute 10 percent of all animal biomass in the tropics and Africa with more than 1000 species, and has the richest intercontinental diversity (Oibiokpa *et al*., 2017). The botanical classification of termite is shown in Table 2.1.

Termites are also a delicacy in the diet of many human cultures and are used in a variety of many traditional medicinal preparations (Kinyuru *et al*., 2016, Shockley and Dossey, 2017). The infraorder name is derived from the Greek word siso (equal) and ptera (winged), which refers to the nearly equal size of the fore-and hind-wings. The name "termite" was derived from the Latin and Late Latin word termes ("woodworm, white ant"), altered by the influence of Latin terere ("to rub, wear, erode") from the earlier word tarmes. Termite nest were commonly known as termitarium or termitaria. In early English, termites were known as wood ants or white ants. The modern term was first used in 1781. Most termites use soil, together with saliva and faeces, to construct their nests (Woodmansey *et al*., 2017). Nest may be subterranean, epigeal (mounds) or within or attached to the outside of shrubs and trees. Some termite nests are simple constructions and their internal microclimate is not much different from that in the soil (Caroll *et al*., 2019). Other nests are often complex structures where temperature and humidity are closely regulated to produce a favorable environment. Above-ground nests are continually being eroded and reconstructed, which redistributes soil

over the surface. The resultant disturbance of soil profiles, changes in soil texture and changes in the nature and distribution of organic matter appear to be more significant than changes in the chemical properties (Omar *et al*., 2017).

The size of the mounds, usually range up to 5 m high and 20 m broad; depends largely on the kind of soil and climatic conditions, while the proximity of the mounds to each other depends not only on the size of the soil type and depth of soil (Dobermann *et al*., 2017). It is not uncommon for the number of mounds to average one and a half per acre (3.7 per hectare).

Table 2.1 Botanical Classification of *Macrotermes bellicosus*

Taxonomic Group	**Animal**
Kingdom	Animalia
Phylum	Arthropoda
Class	Insecta
Order	Isoptera
Family	Termitidae
Genus	*Macrotermes*
Species	*bellicosus*

Source: shahar, (2018)

2.2 Ethno-Medicinal Uses of Termites

The use of termites for medicinal purposes is common especially in the rural parts of the world Latunde-Dada *et al*. (2016) examined the use of termites for medicinal purpose by analysing several literature reviews. Their findings showed that approximately 45 species of termites from four families are used all over the world, with 43 species being part of human diet and livestock feeds. Nine termite species were recorded to be used for therapeutic purposes. Africa is the continent with the highest number of usage followed by America and Asia respectively. *Macrotermes bellicosus* is locally used in Nigeria to treat wounds, sickness of pregnant women and as charm for spiritual protection (Jongema, 2017).Termites (*Macrotermes termitidae*) are used to cure haemorrhage. The mound is used in combination with the bark of the muton (a tree with red bark). The bark is removed and is placed in a broken pot and mixed with the termite mound. The patient is given the mixture to drink in small quantity. The mound can also be mixed with wild leaves to cure haemorrhagic wounds (lbuquerque and Rômulo, 2016).

Macrotermes exiguus contains antiviral properties used for effective treatment of cold, cough, sore throat, flu, whooping cough, catarrh, bronchitis, sinusitis and asthma (Riggi et al., 2016). Kaolin a medicinal clay substance from termite mounds is used in local medicine for treating gastric disorders such as dysentery, swelling of large intestine, indigestion, stomach ache, diarrhoea and mumps (fungal infection) (Amadi and Kiin-Kabari, 2016). A study showed that *Odontotermes formosanus* can be used for treating ulcer and it was also reported that *Odontotermes formosanus* possess analgesic properties and as such can be effective for treating pain and rheumatism (Van Huis, 2017). It is reported that products isolated from

termites such as peptides, espinigerin and termicine showed antifungal properties especially in the treatment of mumps in men.

2.3 Diabetic Foot Infections

Diabetic foot infections (DFI) are a common complications of poorly controlled diabetes, forming as a result of breaking down of skin tissue and exposing the layers underneath. They are most common under the toes and the balls of the feet and the bones found in these foot region (Odusan *et al*., 2017). A recent update suggests that nearly 2 out of every 10 out-patients with diabetes in Nigeria have diabetic foot disease and DFU (Diabetic foot ulcer) accounts for nearly a third of diabetes-related hospital admissions. The most unpleasant potential consequence of DFI besides death is lower extremity amputation (LEA) (Anumah *et al*., 2017).

2.3.1 Epidemiology of diabetic foot infections

It is estimated that a person with diabetes has up to 25 % chance of developing DFI in his or her life- time. The burden of DFI is high both in Africa generally and in Nigeria in particular. A recent update suggests that nearly 2 out of every 10 out-patients with diabetes in Nigeria have diabetic foot infections (Richard *et al*., 2017) and DFI accounts for nearly a third of diabetes-related hospital admissions. Diabetic foot infection is associated with prolonged hospital stay, substantial economic burden and high mortality (Akkus *et al*., 2016). More than three-quarters of all LEAs performed in people with diabetes is secondary to DFI which is currently the leading cause of non-trauma related LEA globally. The negative medical and psychosocial consequences of LEA in people with DM are substantial. About 10% of those who suffer major LEAs die intra- admission (Roy *et al*., 2019). And post LEA survivors have

a significantly reduced quality of life and higher risk of depression which may be related to impaired psycho-social functioning. The long term prognosis after DFI-related LEA is also reportedly abysmal, with 3-year mortality after diabetic foot amputation ranging from 35 to 50 % (Sadriwala *et al*., 2018). In fact, long term prognosis after major LEAs in people with diabetes has been shown to be comparable to breast and prostate malignancies in females and males respectively. Diabetes-related

LEA rates have significantly declined in many Western countries (Narayan and Kelly, 2016). This is however not the case in many parts of Africa where DFI-related LEA rates are still very high. Less than half a decade ago, amputation rate as high as 52 % was reported among patients hospitalized for DFI in one tertiary healthcare center in Nigeria. Efforts to prevent this unpleasant scenario therefore deserve utmost attention, and this could be partly accomplished by risk factor identification (Hoffmann *et al*., 2016).

2.5 Causative Agents of Diabetic Foot Infection

Staphylococcus aureus and ß-hemolytic streptococci are the first microorganisms to colonize and acutely infect breaks in the skin. Chronic wounds develop a more complex poly-microbial microbiology, including aerobic Gram-negative rods and anaerobes. Gramnegative bacilli, mainly Enterobacteriaceae, are found in many patients with chronic or previously treated infections, and *Pseudomonas aeruginosa* is specifically associated with wounds treated with wet dressings (Omar *et al*., 2017). Less virulent bacteria such as *Enterococcus* spp, coagulase-negative *Staphylococcus* spp, or *Corynebacterium* spp. may also represent true pathogens. Anaerobes are rarely the sole pathogen, but they often participate in a mixed infection with aerobes, especially in cases of deep tissue infection.

These mixed infections provide an optimal opportunity for microbial synergy, which increases the net pathogenic effect and hence the severity of infection (Hamsa *et al*., 2019). Assuming the qualitative microbiology remains constant, the probability of wound infection increases as the microbial load increases to a critical level. At this level, infection or a failure to heal is considered almost inevitable. There are exceptions to this rule of thumb, however, as various organisms have different intrinsic virulence potentials. A good example is ß-hemolytic streptococci which is able to induce tissue damage at 102 CFU/g of tissue, while greater counts of less pathogenic organisms may be of little clinical significance (Wang *et al*., 2017).

A third critical factor is the efficacy of the host's immune response in dealing with wound microflora. In DFI, infection is facilitated by intrinsic immunological deficits, especially in terms of neutrophil dysfunction (Kelkawi *et al*., 2017). Notwithstanding, infection is also facilitated by local potentiating factors such as tissue necrosis, hypoxia (due to poor local perfusion accentuated by the hypermetabolic state and microbial cellular metabolism), ischemia, and the particular anatomy of the foot (i.e., it is divided into several compartments, explaining the rapid spread of infection), all of which impair immune cell activity in the wound environment (Caroll *et al*., 2019).

Pseudomonas aeruginosa is a common bacterium, Gram-negative opportunistic pathogen capable of infecting humans with compromised natural defenses and causing severe pulmonary disease. It is one of the leading pathogen associated with nosocomial infections. It has a vast arsenal of pathogenicity factors that are used to interfere with host defenses (Jadhav, *et al*., 2016). Pathogenesis in *P. aeruginosa* facilitates adhesion, modulate or disrupt host cell pathways, and target the extracellular matrix. The propensity of *P. aeruginosa* to form biofilms further protects it from antibiotics and the host immune system. The organism

is intrinsically resistant to a large number of antibiotics and can acquire resistance to many others, making treatment difficult. It provokes a potent inflammatory response during the infectious process. The majority of mortalities in immunocompromised patients; cystic fibrosis, can be attributed to the progressive decline of lung function resulting from chronic infection by pathogens such as *P. aeruginosa* (Franchi *et al*., 2020).

Antibiotic treatment of chronic *P. aeruginosa* infections may temporarily suppress symptoms; however, they do not eradicate the pathogen. Lung diseases caused by *P. aeruginosa* are a leading cause of death in immunocompromised individuals as well as in children. Although immunocytes recruitment is critical to augment the host defense, excessive neutrophil accumulation results in life-threatening diseases, such as acute lung injury, as well as acute respiratory distress syndrome (Döring *et al*., 2016).

Several virulence factors have been studied for their roles as potential vaccine candidate, although there is currently no clinically accepted vaccine. Understanding host-pathogen interaction is critical for the development of effective therapeutic strategies to control the damage in the lung.

2.4 Pathogenesis and Major Virulence Factors

2.4.1 Pathogenesis of *Pseudomonas aeruginosa* as a common bacteria associated with Diabetic foot infection

Pathogenesis in *P. aeruginosa* is mediated by multiple bacterial virulence factors that facilitate adhesion and/or disrupt host cell signaling pathways while targeting the extracellular matrix in Figure 1, *P. aeruginosa* stands out as a unique and threatening organism as it is capable of causing severe invasive disease and of evading immune defenses causing persisting infections that are nearly impossible to eradicate. The subsequent tissue damage, invasion, and dissemination of *P. aeruginosa* are likely attributed to the many

virulence factors it produces. These virulence factors play an initial role in motility and adhesion to the epithelium. These virulence factors are thought to be critical for maximum virulence of *P. aeruginosa*; however, based on observations of diverse plant and animal models, the relative contribution of any given factor may vary with the type of infection (Wei and Ma, 2018).

Several of these virulence factors have also been studied for their roles as potential vaccine candidate although there is currently no general accepted vaccine. The following section briefly outlines several prominent putative virulence factors produce by *P. aeruginosa* and their proposed roles in contributing to disease. The lipopolysaccharide is a predominant component of the outer membrane of *P. aeruginosa* (Serra *et al*., 2017). Bacterial LPS typically consist of a hydrophobic domain known as lipid A (or endotoxin), a non-repeating core oligosaccharide, and a distal polysaccharide (or O-antigen) (Leslie *et al*., 2016). The composition of O-antigen determines the serotypes of the *P. aeruginosa* isolate and currently there are 20 serotypes based on serological reactivity of the O-antigen.

Lipopolysaccharide plays a prominent role in activation the host's innate and adaptive (or acquired) immune responses; and, eventually causes dysregulated inflammation responses that contribute to morbidity and mortality (Rada *et al*., 2016).

Recognition of LPS occurs largely by TLR4–MD2–CD14 complex, which is present on many cell types including macrophages and dendritic cells. Recognition of lipid A also requires an accessory protein, LPS-binding protein (LBP), which converts oligomeric micelles of LPS to a monomer for delivery to CD14, which has high-affinity membrane protein that can also circulate in a soluble form. In addition, NLRs regulate both inflammation and pyroptosis (Lipsky *et al*., 2016).

The NLRP1 inflammasome was first described in 2002 in human monocytes as a molecular compound that responds to LPS (Hatipoglu *et al*., 2016). Many stimuli that trigger assembly of the inflammasomes have been described. LPS has been reported to activate NLRP3 when administered in the presence of ATP as well as NLRP2. A number of LPS vaccines have been investigated for use in CF patients in phase II and III clinical trials; however, these have not been successful (Doring and Pier, 2016). The LPS based vaccines provides little immunity and did not appear to protect the patients from infection with *P. aeruginosa*.

2.4.2 Pathogenesis of *Staphylococcus aureus*

The knowledge of *S. aureus* pathogenecity reveals that these bacteria seem to be adapted for soft tissue and bone infection. Majority of infections remain localized to the feet.

Generally, systemic infection secondary to diabetic foot is less prevalent (around 10%).

This becomes particularly noticeable when analyzing infection process (Periasamy *et al*., 2017). The first defense against *S.aureus* infection is the neutrophil response. When *S.aureus* invades the compromised skin, neutrophils and macrophages migrate to the site of infection. *Staphylococcus aureus* evades this response using different methods (e.g, blocking sequestering host antibodies, chemotaxis of leukocytes, hiding from detection via capsule or biofilm formation and resisting destruction after ingestion by phagocytes)

(Lavigne *et al*., 2017).

2.4.2.1 *Staphylococcus aureus* toxins in diabetic foot infection

The ability of *S. aureus* to cause diabetic foot infection is defined by numerous virulence factors among which secreted toxins play an important role (partcipating in colonization, persistence, evasion of the immune system and dissemination) (Vandenesch *et al*., 2016).

These toxins include the pore-forming toxins, the exfoliatins, the superantigen exotoxins (SAg) and the EDIN (epidermal cell differentiation inhibitors) toxins. These cytolytic toxins

can damage membranes of host cells leading to cell lysis. Haemolysins lyse red blood cells, while leukotoxins targets white blood cells.

Pore_forming toxins

Pore-forming toxins (PFT) of S. aureus through pore-forming and pro-inflammatory activity have the abilty to lyse host cells. They include the single-componet α-toxin (or αhaemolysin) and phenol-soluble modulins (PSMs) and bi-component leukotoxins including panton-valentine leukocidin (PVL), ɣ-haemolysin and leukocidin D/E (Chatterjee

et al.,

2016).

Alpha toxin

This PFT is a beta_barrel forming toxin, which consists of beta sheets. It is released by the majority of *S.aureus* as a water_soluble monomer. Its targets are red blood cells and leukoc ytes except neutrophils. Although α_toxin is the most frequently secreted, few studies have focused on t he role of this hemolysin produced by *S. aureus* in DFI. In a French national study, almost all the strains harbored the α_toxin encoding gene hla independently of the grade (Otto *et al*., 2018). However, this proportion varies between methicillin-susceptible *S. aureus* (MSSA) and MRSA. The α-hemolysin gene was significantly less present in MRSA (16.4 %) than in MSSA strains (100 %). As we noted previously, DFIs caused by MRSA present a similar severity of infections to MSSA, excluding an increased role of α-toxin in the pathogenicity of MSSA.

Phenol soluble modulins

Recently, the role of a family of secreted peptides, the phenol-soluble modulins (PSMs), has been described in staphylococcal pathogenesis. PSMs are produced by the majority of *S. aureus* strains (Dumont *et al.*, 2011). These toxins are membrane-injuring toxins. They are structurally characterized as a family of seven small amphipathic α-helical peptides. Some PSMs are described: PSMα1–PSMα4 and delta-toxin. Like LukAB (described below), they induce human neutrophil lysis after phagocytosis, a pathogenesis mechanism of great importance for the high toxicity. In DFI, to date, no report has evaluated the significance of these virulence factors in the pathogenicity of *S.aureus* (Liu *et al*., 2016).

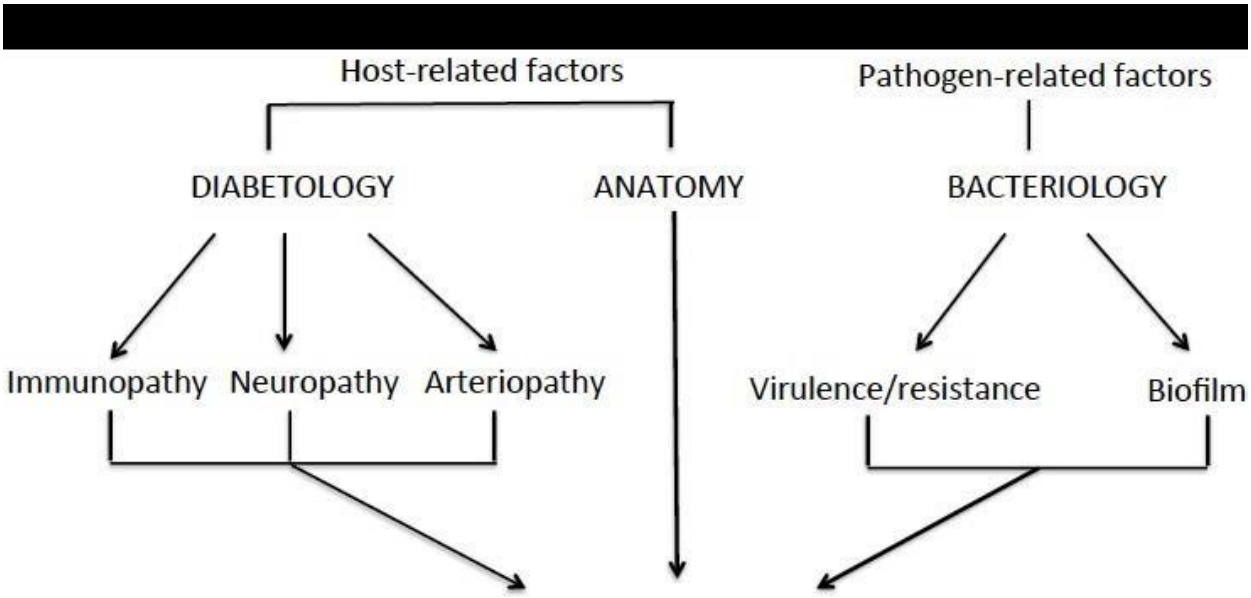

Figure 1: Interactions between metabolic, anatomical and bacteriological factors in diabetic foot infection.

2.4.3 Pathogenesis of *Klebsiella pneumoniae*

Klebsiella pneumoniae, a member of the family *Enterobacteriaceae*, is a rod-shaped, Gramnegative, lactose-fermenting bacillus with a prominent capsule. Typical *K. pneumoniae*

is an opportunistic pathogen that is widely found in the mouth, skin and intestines, as well as in hospital settings and medical devices. Opportunistic *K. pneumoniae* mostly affects those with compromised immune systems or who are weakened by other infections such as DFI. Infections caused by *K. pneumoniae* tend to be chronic due to the two following major reasons: *K. pneumoniae* biofilms formed in vivo protect the pathogen from attacks of the host immune responses and antibiotics (Zia *et al*., 2017), and nosocomial isolates of *K. pneumoniae* often display multidrug-resistance phenotypes that are commonly caused by the presence of extended-spectrum β-lactamases or carbapenemases, making it difficult to choose appropriate antibiotics for treatment.

2.4.3.1 *Suppression of early inflammatory response*

Airway epithelial cells produce Toll-like receptors (TLRs) in order to recognize conserved molecules expressed by pathogens, which in turn activate signaling pathways for producing antimicrobial molecules, such as human β-defensins and co-stimulatory molecules and for releasing cytokines and chemokines. In sharp contrast to the infection of wild-type capsulated *K. pneumoniae* strains that characteristically lack early inflammatory response, avirulent CPS mutants activate a potent inflammatory program. Mechanistically, the anti- inflammatory effect of CPS is characterized by inhibition of IL-8 expression through inhibiting TLR2 and TLR4 signaling and NOD1-dependent pathways (Regueiro *et al*.,

2018).

2.4.3.2 *Outer membrane porins*

Klebsiella pneumoniae produces two major outer membrane porins-OmpK35 and OmpK36-through which hydrophilic molecules (e.g., nutrients and

cephalasporins/carbapenems) diffuse into the bacteria. In addition, *K. pneumoniae* expresses alternative porins, such as KpnO and OmpK26, in order to compensate for the absence of

OmpK35/36 (Garcia-Sureda *et al*., 2016). Loss of any of OmpK36, KpnO or OmpK26 leads to increased resistance to cephalosporins/carbapenems and reduced virulence in mouse models of acute systemic infections, while loss of OmpK35 has no effect on antibiotic resistance and virulence. Loss of OmpK36 remodels the surface structure of *K. pneumoniae* and thereby alters the binding of phagocytes, leading to increased susceptibility to phagocytosis thus, a attenuation in virulence (Figure 1).

2.4.3.3 *Efflux pumps*

Klebsiella pneumoniae expresses the efflux pump AcrAB, which contributes to the export of not only antibiotics (e.g., quinolones and β-lactams), but also host-derived antimicrobial agents (e.g the antimicrobial agents present in human bronchoalveolar lavage fluid and human antimicrobial peptides and AcrAB acts as a determinant of *K. pneumoniae* resistance to host innate immune defenses. The inactivation of AcrAB not only leads to a multidrug resistance phenotype, but also to a reduced capacity to cause pneumonia in a murine model. The expression of another *K. pneumoniae* efflux pump is not related to any antibiotic resistance phenotype, but it confers acid tolerance in vitro and high competition potential in the host (Padilla *et al*., 2016).

2.5 Silver Nanoparticles

Silver nanoparticles (AgNPs) have been used for decades as anti-bacterial agents in various industrial fields such as cosmetics, health industry, food storage, textile coatings and environmental applications, although their toxicity is not fully recognized yet (Reginold *et al*., 2016). Antimicrobial and catalytic activity of AgNPs depends on their size as well as structure, shape, size distribution and physico-chemical environment. The unique prroperties of AgNPs require novel or modified toxicological methods for evaluation of their toxic

potential combined with robust analytical methods for characterization of nanoparticles applied in relevant vehicles, e.g., culture medium with/without serum and phosphate buffered saline (Pérez-Herrero and Fernández, 2017).

2.6 Combined Therapy of Silver Nanoparticles and Insects Extract

In recent years, the combination therapy of multiple drugs has been considered an effective strategy for DFI treatments by achieving synergistic therapeutic efficacy and reducing drug side effect (DeSantis *et al*., 2016). Due to its low cytotoxicity, AgNPs were considered particularly attractive for the production of a new class of antimicrobials thereby opening up a completely new way to combat a wide range of bacterial pathogens in combination with (Biel *et al*., 2016). In fact, the potent antibacterial and broad-spectrum activity against morphologically and metabolically different microorganisms seems to be correlated with a multifaceted mechanism by which nanoparticles interact with microbes (Dos Santos *et al*., 2017).

It is likely that a combined effect between the activity of the nanoparticles and free ions from insects' extracts contributes in different ways to produce a strong antibacterial activity of broad spectrum. Moreover, their particular structure and the different modes of establishing an interaction with bacterial surfaces may offer a unique and under probed antibacterial mechanism to explore (Muhammad *et al.*, 2016). From a structural point of view, AgNPs have at least one dimension in the range from 1 to 100 nm and more

importantly, as particle size decreases, the surface area-to-volume ratio greatly increases. As a consequence, the physical, chemical and biological properties are markedly different from those of the bulk material of origin (Siddiki *et al*., 2018). The AgNPs are able to physically interact with the cell surface of various bacteria. This is particularly important in the case of

Gram-negative bacteria where numerous studies have observed the adhesion and accumulation of AgNPs to the bacterial surface.

Many studies have reported that AgNPs can damage cell membranes leading to structural changes, which render bacteria more permeable. This effect is highly influenced by the nanoparticles' size, shape and concentration and a study using *Escherichia coli* confirmed that AgNPs accumulation on the membrane cell creates gaps in the integrity of the bilayer which predisposes it to a permeability increase and finally bacterial cell death (Dehghanizade *et al*., 2018). Several studies have shown that AgNP activity is strongly dependent on the size. Infact, the bactericidal activity of AgNPs of smaller dimensions (<30 nm) was found to be optimal against *Streptococcus pyogenes* and *Klebsiella pneumoniae*. Smaller nanoparticles seem to have a superior ability to penetrate into bacteria.The interactions with the membranes and any resulting damage, which may lead to cell death, are certainly more evident in the case of nanoparticles with smaller diameter and a positive zeta potential (Wu *et al*., 2017). Electrostatic forces that develop when nanoparticles with a positive zeta potential encounter bacteria with a negative surface charge promote a closer attraction and interaction between the two entities and possibly the penetration in bacterial membranes. Indeed, the zeta potential along with the size of the nanoparticles is a fundamental parameter for controlling the antimicrobial activity and more effective nanoparticles have a positive zeta potential and a reduced size (Manikandan *et al*., 2017). The use of combination strategies of insects' metabolites and silver nanoparticles for combating antibiotic resistance is slowly finding its way as a promising attempt to reduce the amount of antibiotics to be administered, therefore lowering the chances of steady resistance development.

2.7 Silver Nanoparticles Anti-biofilm Activity

As reported before, the number of infections associated with antibiotic-resistant bacteria is continuously increasing. Microorganisms growing in biofilms cause many of these infections. The most common biofilm-forming bacteria associated with human infections are: *E. faecalis, S. aureus, S.epidermidis, Streptococcus.viridans, E.coli, K.pneumoniae, Moraxella catarrhalis, Proteus.mirabilis* and *P.aeruginosa* (Rai *et al*., 2016). Biofilms may be one of the leading causes for a shift from acute-phase diseases to chronic diseases. Most common diseases involving bacteria able to form biofilm are diabetic foot and biliary tract infections, cystic fibrosis, dental caries, endocarditis, otitis and periodontal diseases. Moreover, several infections may be associated with foreign body material such as contact lens, sutures, artificial heart valves, arteriovenous shunts, catheters and orthopedic prostheses (Aderibigbe, 2017). The sites of infections may be different but the characteristics (mechanism for biofilm formation and development of resistance) of the causative agent are similar.

Biofilms are communities of microorganisms attached to a solid surface. These adherent cells are frequently embedded within a self-produced matrix of extracellular polymeric substance. Biofilm extracellular polymeric substance is a conglomeration composed of DNA, proteins and polysaccharides. The matrix is produced under the control of enzymes secreted in response to nutrient availability (Teow *et al*., 2018). One of the first reports on the antibiotic effect of AgNPs on *P.aeruginosa* and *S.epidermidis*, and their effect on biofilm formation, was produced by Kalishwaralal *et al.* (2016). The study focused on two important pathogens causing keratitis and the effect of a 2 h of treatment with AgNPs at a concentration of 100 μM showed that a 95% and 98% decrease of the biofilm was obtained. Therefore the authors concluded that AgNPs are able to induce the detachment of *P.aeruginosa* and *S.epidermidis*

with rapidity and efficiency, opening clinical possibilities of alternative therapies. An important feature to evaluate the real efficiency of the nanoparticles is derived from the chosen stabilization method employed.

To this regard several coatings and chemicals have been reported: (i) starch was successfully employed to prepare AgNPs which had a disrupting effect on biofilms produced by *P. aeruginosa and S. aureus* (Rajakumar *et al*., 2017). (ii) citrate-capped AgNPs of various sizes were shown to inhibit *P.aeruginosa* PAO1 biofilms. (iii) polyvinylpyrrolidone (PVP) showed good antibacterial activity towards *S.aureus, E.coli, P. aeruginosa, Bacillus subtilis*. (iv) β-cyclodextrin is also an effective capping and stabilizing agent that reduces the toxicity of AgNPs against the mammalian cell while enhancing their antibiofilm activity. (Mohanty *et al*., 2012) used a simple and environment friendly approach to form stable colloids of nontoxic AgNPs using starch to reduce silver nitrate to silver metal and simultaneously stabilized the nanoparticles in starch solution. Then they tested the effect of AgNPs on biofilm formation by *P.aeruginosa* and *S.aureus* with varying concentrations of AgNPs. Longer treatments (48 h) increased the antibiofilm efficiency to approximately 65 % and 88 % reduction in biofilm formation at micromolar concentrations. The ability to disrupt *P.aeruginosa* biofilm formation after treatment with the antimicrobial peptide LL-37, already known to impair biofilm formation, and AgNPs was also analysed and, in comparison to LL-37, treatment with AgNPs resulted in a 3-fold reduction of biofilm formation. Multidrug resistant (MDR) strains of *P. aeruginosa* were treated with AgNPs to investigate the eventual increased resistance compared to sensible strains. In the multi-drug resistant strains, the inhibition rate of AgNPs was highest at concentration of

20μg/mL similarly to the parental strain. Therefore biofilms derived from multi-resistant bacteria do not show increased resistance to silver (Gupta *et al*., 2016).

CHAPTER THREE

3.0 MATERIALS AND METHODS

3.1 Materials

Olympus Microscope, Vertical pressure steam sterilizer, Culturingbox- biochemical, Shp 200, Whatman filter paper (England), Weighing balance, ottans pioneer, MacConkey Agar, Nutrient Agar, Nutrient broth, Peptone water, Eosine methylene blue (Titan Biotech Limited, Rajasthan, India), Ethanol, N-Haxane, Ethyl acetate, plain sample bottles (JHD, China), Glass wares - UK, cotton wool, foil paper, wire loop, JSM needle and syringe, Amitch swab stick (PACPRO Industries limited Lagos, Nigeria), Hand gloves- unigloves (Thailand), Ferric chloride, sodium hydroxide, normal saline, tryptone broth, hydrochloric acid,

Dragendroff''s reagent, sulphuric acid, chloroform, acetic anhydride, Nitric acid (sigma product, JHD, China), Hydrogen peroxide, normal saline, distilled water, Kovac's reagent, citrate agar, oxidase reagent, methyl red reagent, vogues-proskauer medium, kligler iron agar, phenol red lactose, sucrose and fructose broth, glucose fermentation medium and liquid paraffin (Titan Biotech Limited, Rajasthan, India), UV- visible spectrophotometer, Scanning electron microscopy, Energy dispersive spectrophotometer, fourier transformed infrared spectrophotometer and X-ray diffractiometer spectrophotometer (LUCIDEON, Materials Development and Commercialization, USA).

3.2 Study Area

The insect used for this study were collected from Maikunkele, Bosso Local Government Area of Niger State.With its headquarters in Maikunkele. It has an area of 1,592km and a population of 203,134 as projectedin 2019 using the national population census figure of 2006 with 2.5% annual growth.

3.2.1 Collection and Identification of Soldier Termites

Live samples of soldier termites were collected from Termitarium in July, 2019 in Maikunkele, Bosso Local Government Area, Minna, Niger State.Termiterium was sampled to harvest the termites. Soldier termites were transferred into sterile plastic containers and transported to the Laboratory of the Department of Animal Biology, Federal University of Technology, Minna, where the identity of soldier termites was authenticated by Zoologist, Dr. K.A. Adeniyi. Soldier termites were identified as *Macrotermes bellicosus*.Voucher specimens were preserved in the department for future reference. Plate 1 depicts the picture of *Macrotermes bellicosus*.

Plate 3.1: *Macrotermes bellicosus* (Field work)

3.2.2 Preparation of soldier termite samples

The method of Billah *et al*. (2016) was employed in preparation of termite samples. Termites were preserved in methanol (99.9 %) to retain their biochemical and morphological integrity. By means of razor blade, the heads of the termites were removed and placed into sterile containers. The heads were freeze-dried using a freeze dryer (model: LGJ-18) at -20 $^{\circ}$C to 27 $^{\circ}$C. Dried heads of termites were pulverized into fine powder using household blender. The pulverized sample was stored in a sterile container. This process was repeated until 300 g of powdered head of the termites was obtained and labeled.

3.2.3 Exhaustive successive extraction of *Macrotermes bellicosus* metabolites

A modification of Sumatra *et al*. (2017) method was employed for the extraction. The extraction process was carried out in the Vaccine and Drug Discovery Laboratory, Centre for Genetic Engineering and Biotechnology, Federal University of Technology, Minna.Using different solvents (ethylacetate, N-hexane ethanol, and distilled water), the solvents ranging from non-polar, mid-polar to highly polar. A total of 150 g of pulverized *Macrotermes bellicosus* material was weighed and soaked in a conical flask containing 1500 mL of 70 % ethanol for the extraction of crude ethanol for 3 days at room temperature (25 ± 2 °C) where the resulting mixtures was filtered using Whatman No. 1 filter paper to remove solid insect residue.The ethanol residue was further remacerated for 2 to 3 times with fresh ethanol solvent for a total of 6 days to obtain more quantity of ethanol extract mixture which was filtered to obtain a filterate and labelled ethanol crude extract (coded Ec). Eccess ethanol solvent was removed from the filtrate (crude ethanol extract) in vacuo at 50 °C in a Buchi Rotary Evaporator. One quarter (1/4) of crude ethanol extract was removed from the evaporated portion, weighed and freeze dried using model: LGJ-18 freeze dryer at -20 °C to 27 °C to obtain 6.5 g of crude ethanol extract. The Remaining portion of crude ethanol extract was subjected to cold marceration extractive technique using a seperation funnel at room temperature. About 200 mL of the solvents (Distilled water, ethylacetate and N-hexane) were seperately added to the seperating funnel containing the crude portion of ethanol extract in order to obtain various extracts of aqueous extract labelled (Eaq), ethylacetate extract labelled (Eoac) and N-hexane extract labelled (NH) according to their polarity where each extraction process was carried out for 24 h. The extracts were collected in a beaker, subjected to freeze-

drying. Various weights of the dried extracts was obtained using a weighing balance and calculated using the formular:

$$\frac{Weight\ of\ dried\ extract}{Weight\ of\ ground\ powder}\ \text{X}\ 100 \quad (3.1)$$

Extracts were weighed to be 5.2 g of ethanol, 7.5 g of aqueous, 5.0 g of ethylacetate and 3.8 g of N-hexane extracts were obtained respectively. Dried extracts were stored in sterile universal bottles at 4^{o}C in a refrigerator until required for antibacterial sensitivity analysis.

3.2.4 Qualitative screening of bioactive components in *Macrotermes bellicosus*

The presence of bioactive constituents in *Macrotermes bellicosus* extracts were screened for bioactive metabolites which was performed according to the method of Wu *et al*. (2016). Qualitative screening allows the detection and sometimes localization of metabolites in given animal materials. Different tests were applied for the detection of different types of metabolites.

3.2.4.1 *Test for saponin (Foam Test)*

The extract was diluted with 20 mL of distilled water and it was shakened vigorously in a test tube for 15 minutes. A layer of foam was formed which indicated the presence of saponin.

3.2.4.2 *Test for phenols (Ferric Chloride Test)*

Extract was treated with 3 drops of ferric chloride solution. Formation of bluish-black colour indicated the presence of phenols.

3.2.4.3 *Test for flavonoids (Shinoda's Test)*

Extract was treated with 10 % NaOH solution. Forrmation of intense yellow colour indicated the presence of flavonoid.

3.2.4.4 *Test for alkaloids*

Small quantity of the extract was dispensed into a test tube, 1 mL of diluted HCl was added and the mixture was heated gently for 20 minutes. The set up was allowed to cool and filtered. Two drops of Dragendroff's reagent was added to the filterate. The development of a creamy precipitate indicated the presence of alkaloids.

3.2.4.5 *Test for tannins (Ferric Chloride Test)*

Two mililitre of aqueous extract was added to 2 mL of water. Two drops of diluted ferric chloride solution was added. A dark green colouration appeared which indicated the presence of tannins.

3.2.4.5 *Test for cyanide*

Fifteen Millilitre (15 mL) of distilled water was added to 0.1 g of the extract in a test tube. An alkaline picrate paper was suspended over the mixture and held in place by rubber bung. The arrangement was allowed to stand for 18 hours at room temperature (37 $^{\circ}$C). Colour change from yellow to orange indicated the presence of cyanide.

3.2.4.6 *Test for steroids (Salkowski's Test)*

In 2 mL of extract, 2 ml of chlorofoam was added. Equal volume of concentrated tetraoxosulphate (iv) acid (H_2SO_4) was added by the side of the test tube. A red layer of chlorofoam appeared and acid layer of greenish-yellow fluorescent. This confirmed the presence of sterols.

3.2.4.7 *Test for terpenoids*

Two millilitre of extract was added to 2 mL of acetic anhydride. Three millilitre of concentrated tetraoxosulphate (iv) acid (H_2SO_4) was carefully added to form a layer. A reddish-brown colouration of the interface was formed to show positive result for the presence of terpenoids.

3.2.4.8 *Test for proteins (Xanthroproteic Test)*

The extracts were treated with few drops of concentrated nitric acid solution.formation of yellow colour indicated the presence of protein.

3.3 Collection of Clinical Test Strains

Test organisms were clinical strains obtained from the foot ulcer of diabetic patients in General Hospital and Ibrahim Badamasi Babangida Specialist hospital Minna, samples were transported to Vaccine Laboratory, Centre for Genetic Engineering and Biotechnology, Federal University of Technology, Minna. The ethical clearance was also obtained from the same Hospital.

3.3.1 Identification of clinical isolates

Isolation and characterization of the test isolates was carried out using the method of Okoli and Iroegbu. (2005). The bacterial isolates were cultured on sterile nutrient agar (NA) and incubated 37°C for 24 hours and subsequently characterized by sub-culturing onto eosine methylene blue agar (EMBA), McConkey agar (MCA) and blood agar (BA). The resulting isolates were Gram stained and further characterized by means of biochemical tests which included catalase, hydrogen sulphide test, starch hydrolysis, Vogues-Proskauer, indole, coagulase, methyl red, citrate utilization test, and sugar fermentation test.The results of the biochemical tests were compared with those of known taxa. Isolates were maintained on nutrient agar slants at 4 °C until required for further use.

3.3.2 Gram Staining and Microscopy

A thin film of 24 h old culture was prepared on sterile slides and fixed by passing over a gentle flame. Each heat-fixed smear was stained by addition of 2 drops of crystal violet solution for 60 seconds and rinsed with water. The smear was again flooded with Gram's iodine for 30 seconds and rinsed with water. Decolorized with 70 % alcohol for 15 seconds and rinsed with distilled water, which was followed by counter-staining with 1 to 2 drops of safranin for 60 seconds and finally rinsed with water, then allowed to air-dry. Dried smear was viewd under oil-immersion objective lens (×100). Gram positive cells appeared purple and Gram negative cells appeared red.

3.3.3 Biochemical tests for identification of bacterial isolates

These tests are used for the identification of bacterial species basednon the differences in the biochemical activities of diffeent bacteria. Bacterial physiology differs from one type of organism to another. The methods of Cheesebrough and Iroegbu, (2010) were adopted.

3.3.3.1 Coagulase test

Blood serum (0.3 ml) was placed on greeze-free glass slide and the bacterial suspension was mixed using sterile wire loop. Coagulation of bacterial suspension indicated a positive result while absence of coagulation indicated a nagative result.

3.3.3.2 Citrate utilization test

Simmon's citrate agar was inoculated by stabbing agar deep with the test organism and incubated at 37 $^{\circ}$C for 96 h. A change in colour from green to blue indicated a positive result and absence of change in colour indicated a negative result.

3.3.3.3 *Vogues Proskauer test*

Forty eight hours (48 h) old broth culture was used for the test. A 3 ml of 40 % potassium hydroxide (KOH) and 1 ml of 5 % of alcoholic alpha naphtol were added to 10.0 cm^3 of the culture in a test tube and agitated. The development of pink colour after 5 minutes indicated a positive result.

3.3.3.4 *Catalase test*

This was carried out with 0.1 ml of 3 % hydrogen peroxide (H_2O_2) which was added on a clean grease-free glass slide. The test organism from preserved medium was taken with sterile wire loop and emulsified in 3 % hydrogen peroxide. Formation of bubbles was recorded as a positive result, while the absence of bubbles was recorded as a negative result.

3.3.3.5 *Sugar fermentation test*

Triple Sugar Iron Agar (TSI) test was inoculated with test organism using sterile wire loop by stabbing through the centre of the medium to the bottom of the test tube and then streaken on the surface of the agar slant, incubated at 37 °C for 24 h. A change in colour from red to yellow indicated positive result.

3.3.3.6 *Haemolysis test*

Sodium azide blood agar was inoculated with the test culture using sterile wire loop and incubated at 37 ºC for 24 h. After 24 h, production of mucoid, greenish zones (surrounding the colonies) indicated α-haemolysis while pale-white mucoid zones surrounding the colonies indicated ß-haemolysis. The absence of haemolysis was indicative of betahaemolysis.

3.3.3.7 *Indole production test*

The isolates were inoculated into nutrient broth and incubated at 37 ºC for 24 h. After 24 hours, 0.3 ml of Kovac's reagent was added to the culture and agitated. A change in colour from purple to red after one minute indicated a positive result. A negative result was recorded when the indole reagent remain unchanged.

3.3.3.8 *Methyl red test*

Forty eight hours (48 h) old broth culture was used. Addition of 1.0 ml methyl red reagent to 10 cm^3 of the broth culture was added to a test tube. Production of red colour indicated a positive result while production of yellow colour indicated a negative result.

3.3.3.9 *Starch hydrolysis test*

Starch agar was inoculated with the test organism using sterile wire loop. This was incubated at 37 ^{o}C for 24 h. The plate was flooded with iodine solution and left for 5 minutes. After 5 minutes, it was drained. For positive result, the colonies remained colourless after draining the iodine solution and the free medium changed to blue-black for negative result, while the whole plate (including the bacteria colonies) turned blue-black.

3.3.3.10 *Test for hydrogen sulphide production*

The test was carried out by inoculating triple sugar iron agar plates with the test organism using sterile wire loop. This was incubated at 37 $^{\circ}$C for 24 h. Production of a black colour precipitate indicated a positive result while absence of black precipitate indicated a negative result.

3.4 Standardization of Bacteria

The method of National Institute for Pharmaceutical Research and Development, NIPRD (2020) was adopted in standardizing the test organisms. Under asceptic environment, a loopful of 24 hours culture was sub-cultured into 5 ml sterile nutrient broth (NB) and incubated at 37 ^{o}C for 24 h. A 0.2 ml of the overnight culture of each isolate was subcultured into 20 ml of sterile nutrient broth in test tubes and incubated for 3-5 h at 37 ^{o}C to obtain 10^{6} cfu/ml of the culture. A loopful of each standardized culture was read in a spectrophotometre at a wavelength of 600 nm. The turbidity of the test suspension was compared to McFarland Standard (0.5). The standardized culture was used to carrry out antibacterial sensitivity assay.

3.5 Antibacterial Assay of Crude Extracts

The antibacterial activity of each crude extract of *Macrotermes bellicosus* (N-hexane, Ethylacetate, Ethanol and Aqueous) was assayed using agar diffusion method as described

by the Clinical and Laboratory Standards Institute, CLSI (2020). Antibacterial activity of extracts was evaluated against *S. aureus*, *P. aeruginosa*, *E. coli*, *S. pyogenes* and *K. pneumoniae*. Mueller-Hinton agar (MHA) was prepared under asceptic conditions (Autoclave) and allowed to cool at ambient temperature (25±2 °C). About 20 mL of sterilized agar was poured in each Petri dishes and was allowed to solidify, a loopful of the standardized bacterial strains were streaked on the surface of solidified agar. Four (4) holes were bored on each plate asceptically using sterile cork borer (6 mm in diameter). The crude *M. bellicosus* extracts were reconstituted by homogenizing 1 g of each extract in 1cm^3 of tween 70 % of the solvents and subsequently dissolving it in 4 cm^3 of sterile distilled water. A 0.2 mg/mL of reconstituted extracts was added to the holes on the Petridishes containing 20 mL of sterile molten Mueller-Hinton agar and inoculated bacteria, the plates were incubated at 37 °C for 24 h using an incubator, the tests were performed in triplicates and the zones of inhibition were measured in millimetre after 24 h of incubation.

Control plates, which included organism viability control (OVC), medium sterility control (MSC) and extract sterility control (ESC) were made in parallel. The antibacterial activity of each extract was compared with that of Amoxicillin+Clavulanic antibiotic (0.5 µg/mL). Results were interpreted as (+) for plates with visible bacterial growth Absence of activity) and (-) for plates with no visible bacterial growth (Presence of activity).

3.6 Biosynthesis of Extract-mediated AgNPs of *Macrotermes bellicosus*

A 2mM of aqueous solution of silver nitrate ($AgNO_3$) was prepared by dissolution of 0.0358 g of $AgNO_3$ in 100 mL of sterile distilled water. One gramme (1 g) of each extract (crude ethanol, ethylacetate, aqueous and n-hexane) of *Macrotermes bellicosus* was dissolved in 100 mL of distilled water. About 40 mL of $AgNO_3$ solution was dispensed into 10 mL of

crude ethanolic extract solution (4:1 dilution). Fifty millilitre (50 mL) of $AgNO_3$ was further dispensed into 10 ml of each extract solution and stirred homogeneously using a magnetic stirrer at 37 $^{\circ}$C. Sodium hydroxide (NaOH) was added as buffer to stabilize the solution. The reaction for the various extracts and $AgNO_3$ was carried out in direct sunlight for instant biosynthesis of extract-mediated AgNPs within 25 min for each extract. The biosynthesis was monitored by UV–vis spectroscopy which exhibited a sharp surface plasmon resonance (SPR) band at 390, 395, 400 and 410 nm after 25 min of sunlight exposure (Lijun *et al*., 2018).

3.6.1 Characterization of extract-mediated AgNPs

Characterization of the most active extract-mediated AgNPs was done using UV-vis spectroscopy, scanning electron microscopy (SEM), X-ray Diffraction (XRD), Energy Dispersive X-ray Spectroscopy (EDS) and Fourier Transform Infrared Spectroscopy (FTIR) to determine the nature of the capping agents in the extract.

3.6.2 UV-visible Spectroscopy

To observe the optical property of biosynthesized silver nanoparticles, extract was periodically analyzed for UV-vis spectroscopy studies (ELICO U.V.165) at room temperature operated at a resolution of 1 nm between 250 and 800 nm ranges according to Banerjee *et al*, (2014). UV-Vis light was passed through the extract and the transmittance of light by the extract was measured. From the transmittance (T), the absorbance was calculated as A= -log (T). An absorbance spectrum was obtained that showed the absorbance of the compound at different wavelengths. The amount of absorbance at any wavelength was due to the chemical structure of the molecule.

3.6.3 Scanning electron microscopy and energy dispersive X-ray spectrum analysis of extract-mediated AgNPs

Scanning Electron Microscopy analysis relies on the detection of high energy electrons emitted from the surface of the sample (ethylacetate-mediated AgNPs extract) after exposure to a highly focused beam of electrons from an electron gun. This beam of electrons was focused to a small spot on the surface of the extract, using SEM objective lens. The process is effectively described below according to the method of Goldstein *et al*.

(2003).

3.6.4 Procedure for SEM analyis of extract -mediated AgNPs

The analysis was done through the application of a beam of electrons (with high energy) in the range between (100-30.000 electron volts) on the extract. Due to the large size of generated spot image of the extract; which could prevent the formation of a sharp image, therefore, the SEM lenses was used to compress the spot to direct focused electron on the extract. The spot size of most SEM is less than (10 nm) with electrons collected from the final lens which interacted with the extract and penetrated to a depth of (1μm) to generate signals used to produce an image. The image was formed point by point depending on the movement of the scan coil, which caused the electron beam to move to discrete locations in a form of straight lines until a rectangular raster was produced on the surface of the extract.

3.6.5 X-Ray diffraction analysis of extract-mediated AgNPs

X-ray diffraction (XRD) measurement of film of the biologically synthesized silver nanoparticles solution was cast onto glass slides were done on a εMMA diffractometre operating at a voltage of 40 kV and current of 20 mA with Cu K (α) radiation of 1.54187 nm

wavelength. The scanning was done in the region of 2 Ɵ from 20° to 80° at 0.02°/min and the time constant was 2 seconds.

3.6.6 Fourier transform infrared spectroscopy (FTIR) of active extracts-mediated AgNPs

According to the method of Jilie and Shaoning (2007) the reaction mixture of the sample (ethylacetate-mediated AgNPs extract) was centrifuged at 15.000 rpm for 15 min after complete reduction of AgNPs by extract and fractions of *M. bellicosus* to separate silver nanoparticles from biomass or other bio-organic compounds which may interfare in analyzing extract-mediated AgNPs interaction. The silver nanoparticle extract pellet obtained after centrifugation were re-dispersed in water and washed (centrifugation and redispersion) with distilled water and washed for three times. Finally, the sample was dried and grinded with KBr pellets and analized on a Nicolet IR 200 (Thermo electron corp).

3.7 Antibacterial Assay of Extract-mediated AgNPs of *Macrotermes bellicosus*

Experiments similar to the antibacterial assay of crude extracts above were executed with extract-mediated AgNPs. Control plates, which included organism viability control (OVC), medium sterility control (MSC) and extract sterility control (ESC) were made in parallel.

The antibacterial activity of each extract was compared with that of Amoxicillin+Clavulanic antibiotic (0.5 mg/mL). Results were interpreted as positive (+) for plates with visible bacterial growth and negative (-) for plates with no visible bacterial growth. The assays were completed in triplicates. After incubation at 37 °C for 24 hours, the zones of inhibition (ZOI) were measured.

3.7.1 Determination of minimum inhibitory concentration of extract-mediated AgNPs

The minimum inhibitory concentration (MIC) of active crude extracts of *Macrotermes bellicosus* (N-hexane, ethylacetate, ethanol and aqueous) and extracts-mediated AgNPs was determined by micro-broth dilution technique respectively as described by Colins *et al*. (1995). A 1mg/mL of the stock ethylacetate-mediated AgNPs extract) was dispensed into the first test tubes of Mueller-Hinton broth (19 mL) by means of double-fold serial dilution of the broth. Thus, 10.0, 5.00, 2.50, 1.50 0.62 and 0.13 mg/mL concentrations were obtained. A loopful of standardized bacterial stock culture in each test tubes of nutrient broth was inoculated into test tubes containing the extracts. The inoculated tubes were incubated at 37 °C for 24 h. Only test tubes-containing extract that showed activity or susceptibility against the test isolates were used for this research. The MIC was determined and recorded by observing the lowest concentration of the extract that inhibited the growth of susceptible isolates. The MIC is defined as the minimum concentration of

ethylacetatemediated AgNPs that inhibited the growth of bacteria.

3.7.2 Determination of minimum bactericidal concentration of extract-mediated AgNPs

The minimum bactericidal concentration (MBC) of ethyaceate-mediated AgNPs extract was determined using the method of Collins *et al*. (1995). Nutrient agar was sterilized according to the manufacturer's specification and sterilized at 121 °C for 15 minutes in an Autoclave. The sterile molten agar (20 mL) was dispensed in Petri-dishes and allowed to cool under normal room temperature 37 °C and under asceptic conditions and inoculated with the bacterial isolates. Petri-dishes with no visible growth after 24 hours of incubation period were sub-cultured into freshly-prepared sterile nutrient agar and incubated at 37 °C for 24 hours.

The least concentration showing no visible growth on sub-culturing was recorded as the minimum bactericidal concentration.

3.8 Investigation of Wound Healing Activity of Synthesized Extract-Mediated Silver Nanoparticles

The topical toxicity and histopathological studies of extract-mediated silver nanoparticles (extract-AgNPs) was conducted on healthy albino rats using the method of Samiksha *et al*, (2016).

3.8.1 Experimental animals

A total of fifty (50) adult Albino rats (150-200 g) were obtained from Animal house at the School of Life Sciences, Federal University of Technology, Minna, Nigeria. The rats were housed in standard plastic rat cages with stainless steel coverlids and sawdust was used as bedding material and maintained under standard Laboratory conditions. Temperature was maintained at 25±1 °C. The Guidelines for the Care and the Use of Laboratory Animals of the Institute for Laboratory Animal Research Council, USA (2011) was adopted for the care of the animals. Fifty healthy albino rats were divided into 10 groups of 5 animals each. Groups 1 to 6 (Treatment groups) and groups 7 to 10 (control groups). Groups of animals (1 to 7) were starved of food before diabetes induction.

3.9.2 Induction of diabetes mellitus in albino rats

The Albino rats were injected with alloxan monohydrate (150 mg/Kg body weight) in normal saline (0.9 % NaCl) intraperitoneally to induce diabetes mellitus. Diabetes was evidenced by elevated serum glucose higher than or equal to 250 mg/dL. Diabetic animals were with symptoms of frequent urination, irritation and blurred vision (Oluwole, *et al*., 2016, Erhirhie, *et al*., 2017).

Grouping of animals is shown below:

Group 1: Diabetes + Wound + *Streptococcus pyogenes* + Ointment

Group 2: Diabetes + Wound + *Escherichia coli* + Ointment

Group 3: Diabetes + Wound + *Klebsiella pneumoniae* + Ointment

Group 4: Diabetes + Wound + *Staphylococcus aureus* + Ointment

Group 5: Diabetes + Wound + *Pseudomonas aeruginosa* + Ointment

Group 6: Diabetes + Wound + Mixed Organisms + Ointment

Group 7: Diabetes + Wound (Negative control)

Group 8: Wound + Extract (Positive control)

Group 9: Wound + Ointment

Group 10: Shaved Skin + Ointment.

Standard dose of alloxan (150 mg/kg b.w) was ascertained using the formular below:

$$\text{Required dose} = \frac{\text{Weight of animals (g)}}{1000\ \text{g}} \times \text{Standard dose (mg)} \quad (3.2)$$

3.9.3 Excision wound model

The wistar Albino rats weighing (150 to 200 g) were selected and the hair from dorsal thoracic central region was shaved using sterile razor blade and sterilized with 70 % methylated spirit to prevent infection. The anticipated area of the wound was marked on the shaved skin. Wounds were created with the aid of toothed forceps, surgical blades and pointed scissors. The diameter of wound area was measured and allowed to establish for 24 hours before infection with test isolates. Test isolates (*P. aeruginosa, S. aureus, E. coli, S. pyogenes and K. pneumoniae*) were inoculated on the induced wound to elicit infection on the skin of each group of animals (groups 1 to 6) except for control groups (7 to 10). Group 10 was shaved only and was not byt was treated with ointment and used to determine extract safety. A

mixture of the test isolates were infected on group 6 animal wounds. An observation of wound rottening, spreading of wounds, and foul exudates indicated the establishment of diabetic foot infection in the rats after four days of infection. The wounds were treated with extract based ointment. The method of Biswas *et al.* (2016) will be employed in the preparation of ointment base extract. The infected wounds were swabbed and inoculated into fresh agar and incubated at 37° C for 24 hours.

3.9.4 Preparation of ointment base extract

Ointment base extract was prepared by dissolving 2.0 mL of extract in 5 g of petroleum jelly (vaseline) and brown bees wax (3 g) was stirred to formulate a homogeneous mixture (Samiksha *et al.*, 2016).

3.9.5 Treatment of animals

On the 4^{th} day, groups 1 to 6 and groups 9 and 10 (control) animals were treated with the ointment base extract. Swab sticks were used to apply the ointment base extract on the surface of the infected wounds. Group 7 (diabetes + wound) and group 8 (wound induction only) will be used as negative and positive control without treatment with ointment. Contraction of wounds was measured for 14 days with an interval of 2 days using white thread and plastic meter rule. The measurement was carried out by placing the white thread across the wound from one end to another then, placed on the plastic metre rule to determine wound closure size.

3.9.6 Wound contraction measurement

Wound contraction (WC) was calculated as:

$$\text{Percentage wound closure} = \frac{(\text{Initial wound size} - \text{specific day wound size})}{Initial\ wound\ size} \times 100 \qquad (3.3)$$

Epithalization period was monitored by noting the number of days required for Escher (a slough or piece of dead tissue that is cast off from surface of skin ulcer) to fall away, leaving no raw wound behind.

3.9.7 Extract (ointment) safety

Group 10 animals were shaved without wound incision and ointment base extract was applied on the shaved skin to determine the safety of extract.

3.9.8 Histopathological study of wounds

The healed skin tissues from all groups of rats were obtained on the 15th day and processed for histopathological studies. Sample skin tissues were washed in normal saline and fixed in 10 % buffered formalin and blocked with paraffin at 40–60 °C for 24 hours.The skin tissues were properly labelled and placed on tissue cassette, procesed using authomatic tissue processor (SLEEMTP tissue processor). The processing phases consisted of fixation, dehydration, clearing and impregnation. Embedding machine was used to dispense wax into an embedding mould, unto which the processed skin tissues and tissue cassette were placed and allowed to solidify. The solidified skin tissue in the cassette was placed in

MR3500 microtome and tiny sections were cut at 5 μm. The sections of skin tissues were heated over water bath at 3 °C below the melting point of wax. Skin tissue sections were picked using microscopic slides angled at 45 °C to drain accumulated water and dried. The slides were then placed on hot plate and allowed to fix at maintained temperature of 3 °C above the melting point of wax. This was done to ascertain the bond between the skin tissue and the slides and also allowed to be fixed for a minimum of 30 minutes. Thereafter, the slides were stained using Harri's haematoxylin and eosin method and allowed to air-dry. Dried slides were mounted with Distyrene Plasticizer Xylene (DPX) mount and cover slips

and observed under Microscope for any histopathological changes. The micrograph skin tissues were assessed and the results were compared to normal control group micrograph structures.

3.10 Statistical Analysis and Data Evaluation

Data generated were expressed as mean value $\pm$ standard error of mean (SEM). Among groups, comparisons of means will be performed by the analysis of variance (ANOVA) test for statistical significance of differences at $P<0.05$. Mean values were separated by Duncan multiple Range Test (DMRT). All data were evaluated using the statistical pachage SPSS version 25.0.0.0

CHAPTER FOUR

4.0 RESULTS AND DISCUSSION

4.1 Results

4.1.1 Physical characteristics and percentage yield of crude extracts of *Macrotermes bellicosus*

Table 4.1 shows the percentage yield of ethanol, N-hexane, ethylacetate, aqueous and residual extracts of *Macrotermes bellicosus* (Soldier Termite). Aqueous extract had the highest yield at 6.0% followed by ethanol extract at 5.2%, ethylacetate extract (5.0%) while N-hexane extract recorded the least yield at 3.8%.

Table: 4.1: Physical Characteristics of Percentage yield of Crude extracts of *Macrotermes bellicosus*

Extract	Physical Characteristics of *Macrotermes bellicosus* extract				Yield%
	Code	Colour	Texture	Weight (g)	
Crude ethanol	Ec	Chocolate-brown	Gummy	5.20	3.34
N-hexane	Eh	Yellowish-brown	Sticky	3.80	2.07
Ethylacetate	Eaoc	Dark-brown	Sticky	5.00	3.33
Aqueous	Eaq	Dark-brown	Crispy	7.50	4.00

$$\text{Percentage Recovery} = \frac{Weight\ of\ obtained\ extract}{Weight\ of\ animal} \times 100 \quad (4.1)$$

4.1.2: **Bioactive components of crude extracts of *Macrotermes bellicosus***

The bioactive components present in crude ethanol, aqueous, ethylacetate and n-hexane extracts of *Macrotermes bellicosus* are presented in Table 4.2. Cyanide, phytate and proteins are present in all the extracts. Phenols are present in crude ethanol, aqueous and ethylacetate extracts. Flavonoids are present in crude ethanol and aqueous extracts. Saponins are present

in all the extracts except in ethylacetate while tannins, steroids and oxalates were absent in all the extracts.

Table 4.2: Bioactive Components of crude extract of *Macrotermes bellicosus*

Bioactive Components	Extracts			
	Ee	**Eaq**	**Eoac**	**Eh**
Cyanides	+	+	+	+
Phenols	+	+	+	ND
Tannins	ND	ND	ND	ND
Flavonoids	+	+	ND	ND
Saponins	+	+	ND	+
Alkaloids	ND	ND	ND	+
Oxalates	ND	ND	ND	ND
Phytates	+	+	+	+

+: Present, Ee: Extract of ethanol, Eaq: Extract of aqueous, Eoac: Extract of ethylacetate, Eh: Extract of n-hexane, ND: Not detected.

4.1.3: Content of bioactive components of *Macrotermes bellicosus*

Table 4.3 shows the quantities of the bioactive components present in *M. bellicosus* (Soldier termite). Cyanides had the highest quantity (2247.00 µg), followed by saponins (321.25 µg), phytates (165.67 µg), phenols (145.21 µg), alkaloids (23.95 µg), flavonoids (20.96 µg), tannins (16.66 µg) while oxalates had the least quantity (0.43 µg) in bioactive components.

4.1.4: Morphological characteristics and identities of isolates

The characterization and identification of bacterial isolates revealed the strains of *Pseudomonas aeruginosa*, *Staphylococcus aureus*, *Klebsiella pneumoniae*, *Escherichia coli* and *Streptococcus pyogenes* in samples collected from patients with diabetic foot are shown in Table 4.4.

4.4: Morphological Characteristics and Identities of Isolates

Isolates	GR	Shape	OX	CAT	CoA	SH	H_2S	IND	MR	VP	CIT	Sugar fermentation				Heamolysis			Suspected organisms
												L	S	G	F	α	β	γ	
1	G-	Rod	+	-	-	-	-	-	-	+	+	+	+	+	-	-	-	-	*Pseudomonas aeruginosa*
2	G+	cocci	-	+	+	-	-	-	+	+	+	+	+	+	+	-	+	-	*Staphylococcus aureus*
3	G-	Rod	-	+	-	-	+	-	-	+	+	+	+	+	-	-	-	-	*Klebsiella pneumoniae*
4	G-	Rod	-	+	-	-	-	-	+	-	-	+	-	+	+	-	-	-	*Escherichia coli*
5	G+	Cocci	-	-	-		-	-	-	-	-	+	+	+	+	-	-	-	*Streptococcus pyogenes*

VP: Vogues Prauskauer,
L: Lactose fermentation,
S: Sucrose fermentation,
G: Glucose fermentation,
F: Fructose fermentation
SH: Starch hydrolysis test,
β: Beta haemolysis production,
α: Alpha haemolysis production,
γ: Gamma haemolysis production,
H_2S: Hydrogen sulphide production,
MR: Methyl red test,
CoA: Coagulase test
GR: Gram's reaction,
CAT: Catalase test,
CIT: Citrate test,
IND: Indole test,
G+: Gram positive,
G- : Gram negative.
+: Present,
-:Absent.

Table 4.3: Content Bioactive Components of *Macrotermes bellicosus*

Bioactive Components	**Quantity (mg/100 g)**
Phenols	145.21
Flavonoids	20.96
Alkaloids	23.95
Cyanides	2247.00
Phytates	165.67
Oxalates	0.43
Tannins	16.66
Saponins	321.25

4.1.5: Antibacterial Activities of crude extracts of *Macrotermes bellicosus* on Test Isolates

The zone of inhibition produced by aqueous extract on pseudomonas aeruginosa was 7.333 ± 0.577 mm. Ethylacetate extract produced zones of inhibition of 6.667 ± 0.577 mm and 7.00 ± 2.00 mm against *Klebsiella pneumoniae* and *Streptococcus pyogenes* respectively.

Table 4.5a: Antibacterial Activity of Crude Extracts of *Macrotermes bellicosus* against Test Isolates at 200 mg/mL

Isolates	Inhibition Zone Diameter (mm) of extracts				
	Ee	Eaq	Eoac	Eh	AMX
Pseudomonas aeruginosa	0.00 ± 0.00^{a}	7.33 ± 0.58^{b}	0.00 ± 0.00^{a}	0.00 ± 0.00^{a}	18.00 ± 1.00^{c}
Escherichia coli	0.00 ± 0.00^{a}	0.00 ± 0.00^{a}	0.00 ± 0.00^{a}	0.00 ± 0.00^{a}	4.23 ± 1.03^{b}
Klebsiella pneumoniae	0.00 ± 0.00^{a}	0.00 ± 0.00^{a}	6.67 ± 0.58^{b}	0.00 ± 0.00^{a}	20.34 ± 1.17^{d}
Stapylococcus aureus	0.00 ± 0.00^{a}	0.00 ± 0.00^{a}	0.00 ± 0.00^{a}	0.00 ± 0.00^{a}	0.00 ± 0.00^{a}
Streptococcus pyogenes	0.00 ± 0.00^{a}	0.00 ± 0.00^{a}	7.00 ± 2.00^{b}	0.00 ± 0.00^{a}	24.51 ± 1.75^{d}

Values are means ± standard deviation. Values on the same column with different superscripts are significantly different from each other ($p<0.05$).
Ee: crude ethanol extract, Eaq: aqueous fraction, Eoac: ethylacetate fraction, Eh: Nhexane fraction, mm: millimetre, mg/ml: milligram per mililitre.

4.1.6 Characteristics of *Macrotermes bellicosus* extract-mediated Silver Nanoparticles

The formation of silver nanoparticles was confirmed by the appearance of dark-brown colour in the solution (Plate 2). The UV-Visible spectroscopy of the synthesized silver nanoparticles of the extracts are shown in figure 1 indicating the absorbance peak for ethylacetate mediated silver nanoparticles (Eoac-AgNPs) occurred at 410 nm. The scanning electron microscopy (SEM) and energy dispersive spectroscopy (EDS) micrograph image formed a spherical-like morphology and aggregated nanoparticles with considerable variability from one another. The elemental signals of AgNPs were analysed by EDS.

Figure 2 shows the energy dispersive spectrum of Carbon (C)-84.97, Oxygen (O)-12.78,

Sodium (Na)-1,12, Silicon (S)-0.5, Phosphorous (P)-0.1, Sulphur (S)-0.11, Chlorine (Cl)0.08, Potassium (K)-0.61 and Silver (Ag)-0.18 peaks at 0.1, 1.3 and 1.0 KeV were assigned to C,O and Na. Si, P, S, Cl, Ag, and K elements corresponded to weak signals.

The results also confirmed the synthesized silver nanoparticles crystalline structure of AgNPs determined by XRD at distinct diffraction peaks shown in figure 3 indicated the structure of silver nanoparticles as face-centred cubic and had a similar diffraction profiles with numerous intense peaks at 2ɵ (10.00°, 18.20°,29.85°,30.00°, 35.60°,45.00° and 55.65°) and also confirmed the synthesisi of silver nanoparticles. The pattern showed strong diffraction peak at 35.60°. Thus, the silver nanoparticles formed are crystalline in nature.

The fourier transform infrared spectroscopy of extract mediated silver nanoparticles showed the possible biomolecules in the region of 1000 to 4000 cm^{-1} of silver nanoparticles showing functional groups. Figure four (figure 4) shows the transmission peaks at 1080.9, 1453.7, 1744.4, 1181.6 and 752.9 cm^{-1}. A broad and strong band at 1080.9 cm^{-1} corresponded to hydroxyl group (-OH) of phenolic compounds. The band at 1453.7 cm^{-} revealed the presence of alkyl group (C-H). The peak around 1744.4 cm^{-1} is attributed to aldehyde group (C=O). This showed that secondary metabolites are involved in the

synthesis of silver nanoparticles. The peak at 1181.6 cm^{-1} showed the presence of functional group (C-O) stretch, while 752.9 cm^{-1} signified the presence of alkyl halide group (C-CI).

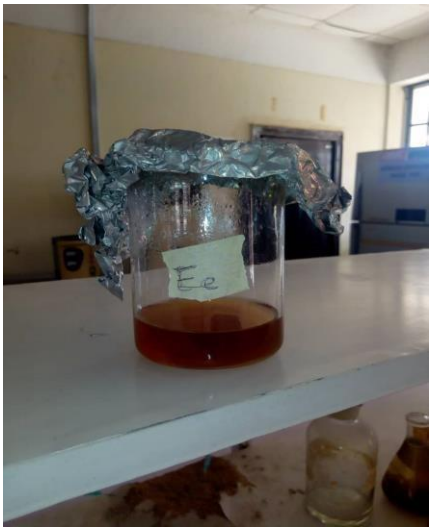

Plate II: Synthesized extracts

Source: Field photograph

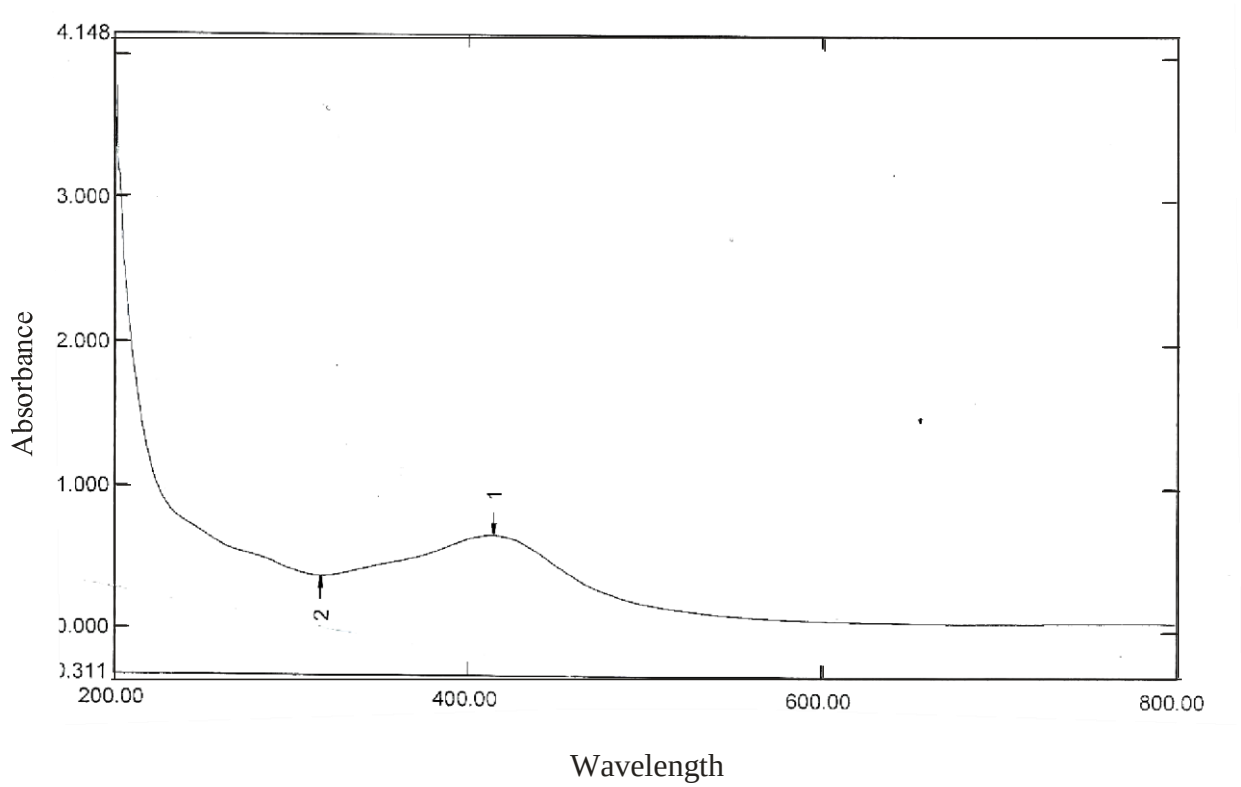

Figure 2: UV-Vis spectrum of extract-mediated silver nanoparticles

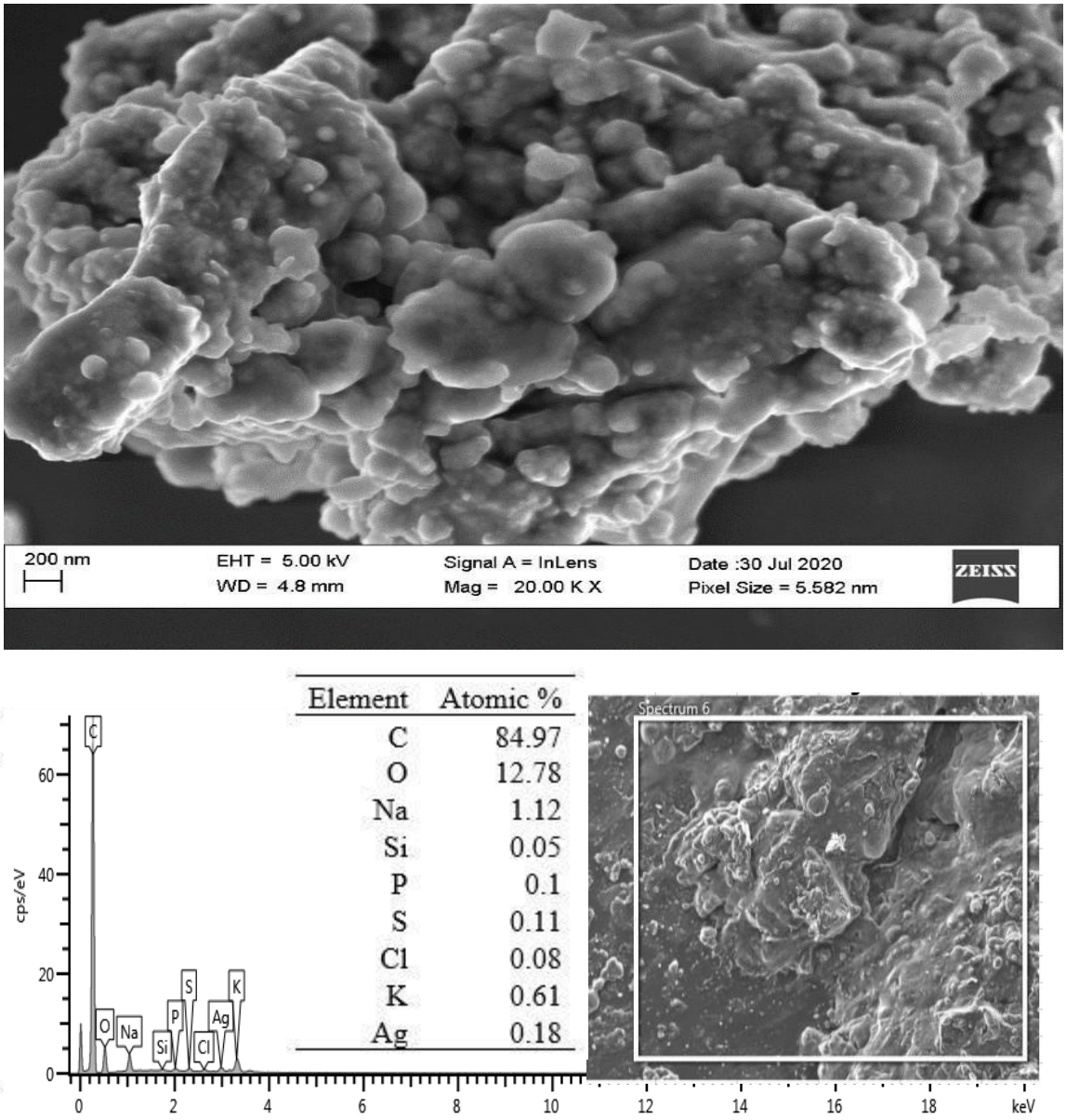

Figure 3: Scanning electron micrograph (SEM) of extract-mediated silver nanoparticles and corresponding energy dispersive spectrum (EDS)

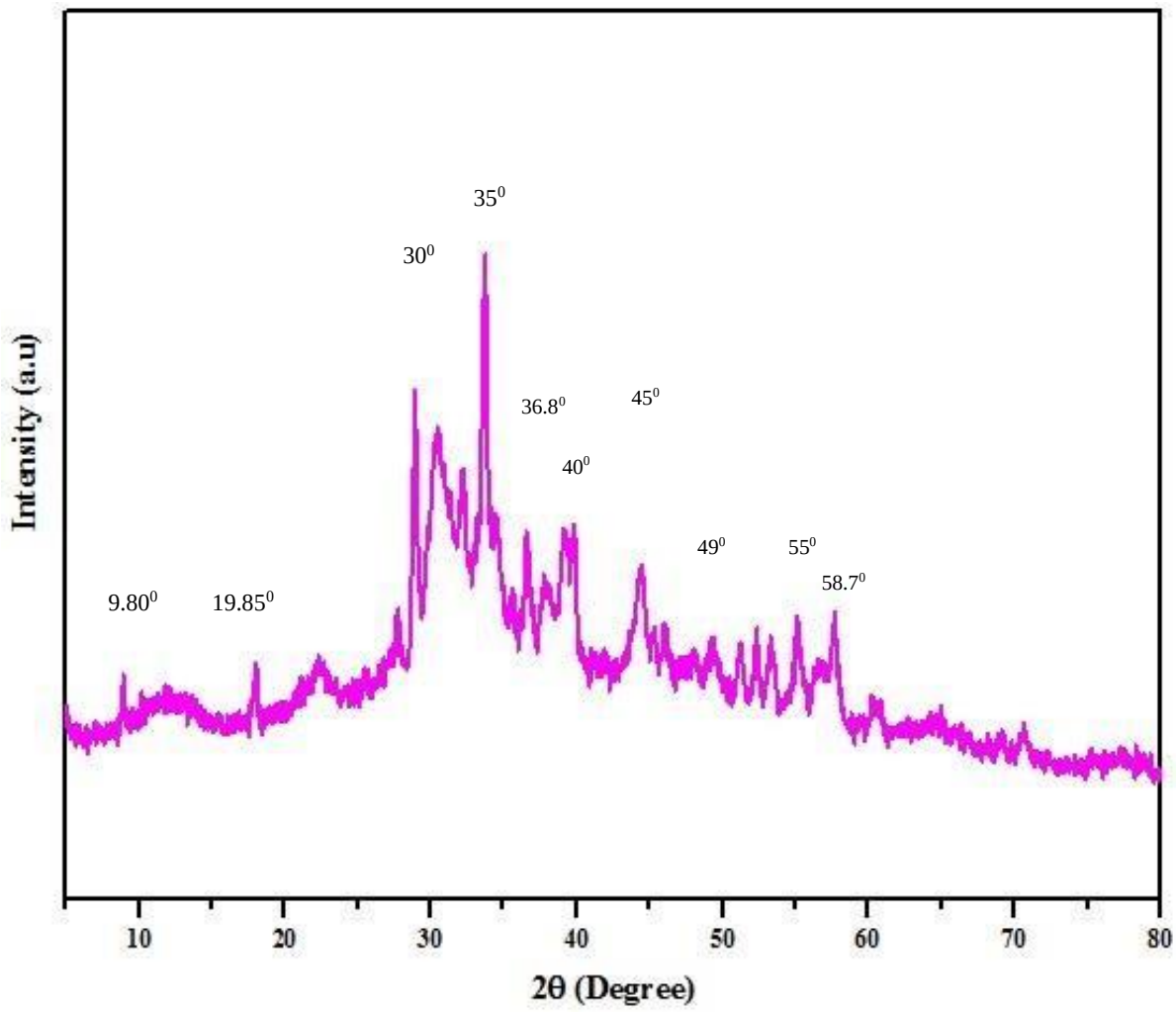

Figure 4: X-ray diffraction pattern of synthesized extract-mediated silver nanoparticles

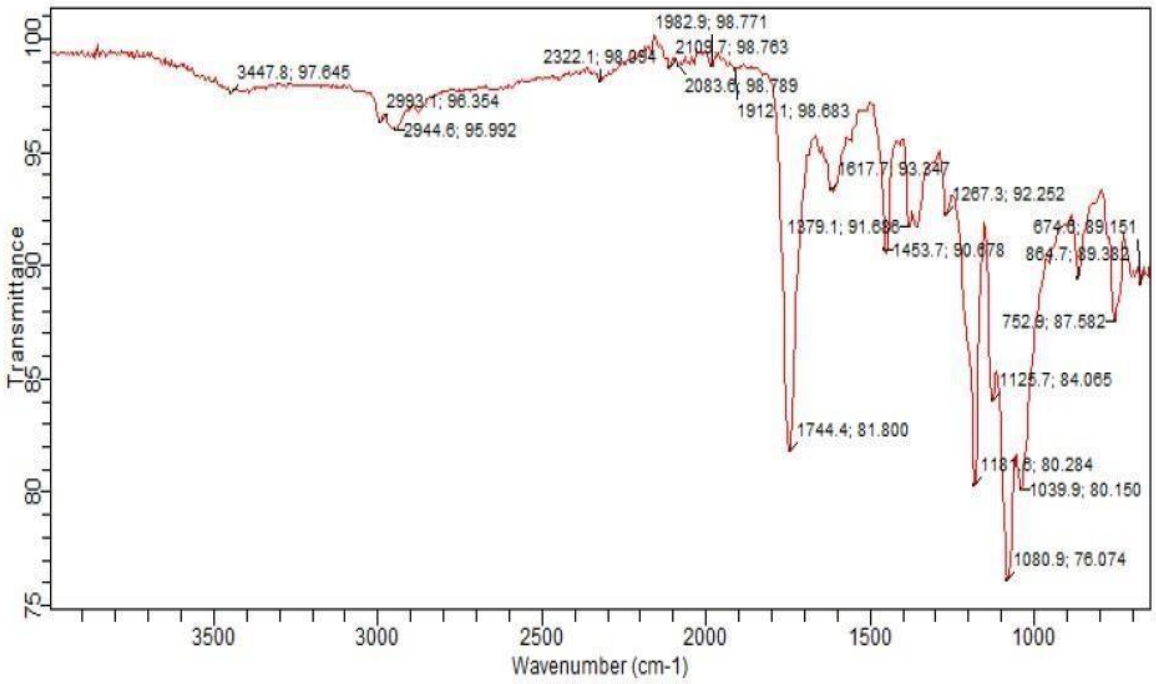

Figure 5: Fourier Transform Infrared (FTIR) Spectroscopy pattern of synthesized extract-mediated Silver Nanoparticles

CHARACTERISTIC INFRARED ABSORPTION BANDS OF FUNCTIONAL GROUPS

Class of Compounds	Absorption, cm^{-1}	Intensity	Assignment
Alkanes and **Alkyls**	2850-3000	s	C-H stretch
	1450-1470	s	C-H bend
	1370-1390	m	CH_3 C-H bend
	1365 + 1395 (two bands)	m	$-CH(CH_3)_2$ or $-(CH_3)_3$ bend
	715-725	w	$-(CH_2)_n$ bend
Alkenes	3020-3140	w-m	=C-H stretch
	1640-1670	vw-m	C=C stretch
$RCH=CH_2$	910 + 990 (two bands)	m + s	=C-H bend
$RR'C=CH_2$	885-895	s	=C-H bend
cis-RCH=CHR'	665-730	m-s, broad	=C-H bend
trans-RCH=CHR'	960-980	s	=C-H bend
RCH=CR'R"	790-840	s	=C-H bend
Alkynes			
R-C≡C-H	3265-3335	s, sharp	≡C-H stretch
	2100-2140	m	C≡C stretch
	610-700	s, broad	≡C-H bend
R-C≡C-R'	2190-2260	vw-w	C≡C stretch
Alkyl halides			
R-F	1000-1350	vs	C-F stretch
R-Cl	750-850	s	C-Cl stretch
R-Br	500-680	s	C-Br stretch
R-I	200-500	s	C-I stretch
Alcohols	3300-3400	s, broad	O-H stretch
$C=C-CH_2-OH$	1035-1050	m-s	C-O stretch
$R-CH_2-OH$ (1°) or C=C-CH(R)-OH	1050-1085	m-s	C-O stretch
RR'CH-OH (2°) or C=C-CRR'-OH	1085-1125	m-s	C-O stretch
RR'R"C-OH (3°)	1125-1205	m-s	C-O stretch
Ar-O-H	1180-1260	m-s	C-O stretch
Ethers			
R-O-R'	1085-1150	s	C-O-C stretch
Ar-O-R	1020-1075 and 1200-1275 (two band)	m-s	=C-O-C sym. & asym. stretch
Aldehydes	2700-2725	m	H-C=O stretch
R-CH=O	1720-1740	s	C=O stretch
C=C-CH=O or Ar-CH=O	1685-1710	s	C=O stretch
Ketones			
RR'C=O	1710-1720	s	C=O stretch
C=C-C(O)-R	1665-1685	s	C=O stretch
Ar-C(O)-R	1675-1695	s	C=O stretch
four member cyclic	1770-1780	s	C=O stretch
five member cyclic	1740-1755	s	C=O stretch
six member cyclic	1710-1720	s	C=O stretch

Class of Compounds	Absorption, cm^{-1}	Intensity	Assignment
Carboxylic Acids	2500-3500	s, broad	O-H stretch
R-C(O)-OH	1710-1715	s, broad	C=O stretch
C=C-C(O)-OH or Ar-C(O)-OH	1680-1710	s	C=O stretch
Esters	aliphatic 1160-1210 acetates ~1240 aromatic 1250-1310	s-vs	O=C-O-C stretch
R-C(O)-O-R	1735-1750	s	C=O stretch
C=C-C(O)-O-R or Ar-C(O)-O-R	1715-1730	s	C=O stretch
R-C(O)-O-Ar	1760-1790	s	C=O stretch
Acyl Chlorides			
R-C(O)-Cl	1785-1815	s	C=O stretch
Ar-C(O)-Cl	1770-1800	s	C=O stretch
Anhydrides			
R-C(O)-O-C(O)-R	~1750 + ~1815	s,s	C=O symmetric
Ar-C(O)-O-C(O)-Ar	~1720 + ~1775 (both two bands)	s,s	& asym. stretch
Nitriles			
R-C≡N	2240-2260	m-s	C≡N stretch
C=C-C≡N or Ar-C≡N	2220-2240	s	C≡N stretch
Amines			
$R-NH_2$	~3400 + ~3500 (two bands)	w	N-H symmetric & asym. stretch
	1580-1650	w-m	N-H bend
RR'N-H	3310-33350	w	N-H stretch
Amides			
$R-C(O)-NH_2$	3200-3400 and 3400-3500 (two bands)	w-m	N-H symmetric & asym. stretch
	1650-1690	s, broad	C=O stretch
	1590-1655	m-s	N-H bend
R-C(O)-NH-R	3400-3500	w-m	N-H stretch
	1640-1690	s, broad	C=O stretch
	1510-1560	m-s	N-H bend
R-C(O)-NR'R"	1630-1680	m-s	C=O stretch
Nitro Compounds			
$R-NO_2$	~1550 and ~1370	s s	N-O symmetric & asym. stretch
$C=C-NO_2$ or $Ar-NO_2$	~1525 and ~1335 (both two bands)	s s	N-O symmetric & asym. stretch
Aromatic Compounds	3010-3100	m	Ar C-H stretch
	1450-1600 (two to four bands)	m-s sharp	ring C=C stretch
monosubstituted	730-770 and 690-710 (two bands)	s s	C-H bend C-H bend
o-disubstituted	735-770	s	C-H bend
m-disubstituted	750-810 and 690-710	s s	C-H bend C-H bend
p-disubstituted	810-840	s	C-H bend

Intensity abbreviations: vw = very weak, w = weak, m = medium, s = strong, vs = very strong

4.1.7 Antibacterial activities of extract-mediated silver nanoparticles at 3.2 mg on test isolates

This result shows the antibacterial activities of the extract-mediated AgNPs at 3.2 mg (Table 4.6) The Ee-AgNPs, Eaq-AgNPs, Eoac-AgNPs, and Eh-AgNPs did not inhibit the growth of *Escherichia coli* and *Staphylococcus aureus* at 80 mg/ml. The Eaq-AgNPs produced zone of inhibition of 7.345 ± 0.577 mm against *Pseudomonas aeruginosa.* The Eoac-AgNPs produced zones of inhibition of 16.000 ± 1.000, 5.000 ± 0.000 mm and 24.000 ± 1.000 mm against *Pseudomonas aeruginosa*, *Klebsiella pneumoniae* and *Streptococcus pyogenes* respectively. The Eh-AgNPs produced zone of inhibition of 4.330 ± 4.004 against *Pseudomonas aeruginosa.*

Table 4.6: Antibacterial Activity of Extract-Mediated Silver Nanoparticles at 3.2 mg on Test Isolates

Isolates	Inhibition Zone Diameter (mm) of Extracts-medi ated AgNPs				
	Ee-AgNPs	**Eaq-AgNPs**	**Eoac-AgNPs**	**Eh-AgNPs**	**AMX**
Pseudomonas aeruginosa	0.00 ± 0.00^{a}	7.35 ± 0.58^{b}	16.00 ± 1.00^{c}	4.33 ± 4.05^{b}	$18.00^{c} \pm 1.00$
Escherichia coli	0.00 ± 0.00^{a}	0.00 ± 0.00^{a}	0.00 ± 0.00^{a}	0.00 ± 0.00^{a}	4.23 ± 1.03^{a}
Klebsiella pneumoniae	0.00 ± 0.00^{a}	0.00 ± 0.00^{a}	6.67 ± 0.58^{b}	0.00 ± 0.00^{a}	20.34 ± 1.17^{d}
Stapylococcus aureus	0.00 ± 0.00^{a}	0.00 ± 0.00^{a}	0.00 ± 0.00^{a}	0.00 ± 0.00^{a}	0.00 ± 0.00^{a}
Streptococcus pyogenes	0.00 ± 0.00^{a}	0.00 ± 0.00^{a}	24.00 ± 1.00^{d}	0.00 ± 0.00^{a}	24.51 ± 1.75^{d}

Values are means ± standard deviation. Values on the same column with different superscripts are significantly different from each other ($p<0.05$).

Ee-AgNPs: ethanol-mediated silver nanoparticles, Eaq: aqueous-mediated silver nanoparticles, Eoac: ethylacetate-mediated silver nanoparticles, Eh: N-hexane-mediated silver nanoparticles, STD Drug: Standard drug, mm: millimetre, mg/ml: milligram per mililitre, AMX: Amoxicillin/Clavulanate.

4.1.8: Antibacterial activities of extract-mediated silver nanoparticles at 8 mg on Test Isolates

Table 4.7 shows the antibacterial activities of extract-mediated AgNPs at 8 mg.The EeAgNPs, Eaq-AgNPs, Eoac-AgNPs, and Eh-AgNPs did not inhibit the growth of *Escherichia coli* and *Staphylococcus aureus* at 3.2 mg did not inhibit the growth of *Staphylococcus aureus* and *Escherichia coli* at 8mg. The Ee-AgNPs produced zone of inhibition of 4.330 ± 4.040 mm against *Klebsiella pneumoniae.* The Eaq-AgNPs produced zones of inhibition of 5.345 ± 0.677 mm and 4.000 ± 1.730 mm against *Pseudomonas aeruginosa* and *Streptococcus pyogenes* respectively. The Eoac-AgNPs produced zones of inhibition of 16.00 ± 1.00 mm, 6.47 ± 0.00 mm and 30.67 ± 2.08 mm against *Pseudomonas aeruginosa, Klebsiella pneumoniae* and *Streptococcus pyogenes* respectively. The EhAgNPs produced zones of inhibition of 16.00 ± 1.73 and 14.00 ± 1.00 against *Pseudomonas aeruginosa* and *Streptococcus pyogenes.*

Table 4.7: Antibacterial Activities of Extract-Mediated Silver Nanoparticle at 8 mg on Test Isolates

Isolates	Inhibition Zone Diameter (mm) of the Extracts- AgNPs				
	Ee-AgNPs	**Eaq-AgNPs**	**Eoac-AgNPs**	**Eh-AgNPs**	**AMX**
Pseudomonas aeruginosa	0.00 ± 0.00^{a}	5.35 ± 0.68^{b}	16.00 ± 1.00^{c}	16.00 ± 1.73^{c}	18.00 ± 1.00^{c}
Escherichia coli	0.00 ± 0.00^{a}	0.00 ± 0.00^{a}	0.00 ± 0.00^{a}	0.00 ± 0.00^{a}	4.23 ± 1.03^{a}
Klebsiella pneumoniae	4.00 ± 1.73^{c}	0.00 ± 0.00^{a}	6.47 ± 0.58^{b}	0.00 ± 0.00^{a}	20.341 ± 1.17^{d}
Stapylococcus aureus	0.00 ± 0.00^{a}	0.00 ± 0.00^{a}	0.00 ± 0.00^{a}	0.00 ± 0.00^{a}	0.00 ± 0.00^{a}
Streptococcus pyogenes	0.00 ± 0.00^{a}	0.00 ± 0.00^{a}	30.67 ± 2.08^{d}	14.00 ± 1.00^{c}	24.51 ± 1.75^{d}

Values are means ± standard deviation. Values on the same column with different superscripts are significantly different from each other ($p<0.05$).

Ee-AgNPs: ethanol-mediated silver nanoparticles, Eaq: aqueous-mediated silver nanoparticles, Eoac: ethylacetate-mediated silver nanoparticles, Eh: N-hexane-mediated silver nanoparticles, AMX: Amoxicillin/Clavulanate, mm: millimetre, mg/ml: milligram per mililitre.

4.1.9: Minimum inhibitory and minimum bactericidal concentrations of extract-mediated silver nanoparticles on test isolates.

The minimum inhibitory and minimum bacterial concentrations of extract-mediated Silver Nanoparticles of *M. bellicosus* on test isolates are shown in Table 4.8. The MIC of the extract against *P. aeruginosa, K. pneumoniae,* and *S. pyogenes* was at 6.25, 25.0, 3.125 mg/cm^3 respectively. Minimum bactericidal concentration for *P. aeruginosa, K. pneumoniae* and *S. pyogenes* was at 12.5, 50.0 and 6.25 mg/ml respectively.

Table 4.8: Minimum Inhibitory and Minimum Bactericidal Concentrations of extract-mediated Silver Nanoparticles on Test Isolates

Isolates	**Concentration of extract-mediated AgNPs (mg/mL)**								
MIC MBC	**200**	**100**	**50**	**25**	**12.5**	**6.25**	**3.125**		
Pseudomonas aeruginosa	+	+	+	+	+	-	-	6.25	12.5
Klebsiella pneumoniae	+	+	+	-	-	-	-	25.0	50.0
Streptococcus pyogenes	+	+	+	+	+	+	-	3.125	6.25

MIC: Minimum inhibitory concentration, MIC: Minimum bactericidal concentration, mg/ml: Milligram per milltre, -: No activity, +: Activity.

4.1.10: Wound healing activity of extract mediated silver nanoparticles

The results of wound healing activities of ointment formulation of extract-mediated Silver Nanoparticles on diabetic-induced Albino rats is as given in Table 4.9.

The infected wounds on the rats' skin were observed to be swollen with foul exudates and gangrene. Initial diameter of wound was measured and recorded at 1.23 ± 0.12 to 1.27 ± 0.30 mm. Treatment of wounds with Eaoc-AgNPs ointment reduced the diameter of the wounds from 0.92 ± 0.30 to 0.33 ± 0.10 mm. There was total wound closure after 14 days in all the treatment groups as compared to the negative control group 8 (Wound+ extract). There was significant ($P<0.05$) wound closure observed from day 8 in most of the treatment groups (group 1 to 6) as compared to group7 (diabetes + wound) which had the highest wound size. Group 8 (wound + Extract) and group 9 (wound only) had the smallest size of wound closure as compared to the treatment groups at day 14.

Table 4.9: Wound Healing Activity of Extract-Mediated Silver

Group	Wound Diameter (mm) at Various Times (Days) 0	2	4	6	8	10	14	
1	1.23± 0.12[a]	1.30±0.15[a]	1.29±0.25[a]	1.24±0.23[a]	0.92±0.3[b]	1.41±0.4[a]	0.80±0.3[b]	0.67±0.25[b]
2	1.29± 0.25[a]	1.24±0.27[a]	1.25±0.25[a]	1.17±0.20[a]	0.10±0.2[b]	0.98±0.1[b]	0.82±0.0[b]	0.72±0.10[b]
3	1.28± 0.43[a]	1.26±0.40[a]	1.20±0.46[a]	1.03±0.55[a]	0.83±0.4[b]	0.8±0.21[b]	0.81±0.2[b]	0.73±0.25[b]
4	1.27± 0.31[a]	1.24±0.35[a]	1.19±0.23[a]	1.12±0.23[a]	0.71±0.3[b]	0.64±0.2[b]	0.52±0.1[b]	0.42±0.10[b]
5	1.25± 0.20[a]	1.22±0.15[a]	1.13±0.20[a]	1.07±0.3[a]	0.71±0.3[b]	0.7±0.12[b]	0.55±0.2[b]	0.43±0.15[b]
6	1.24±0.42[a]	1.21±0.36[a]	1.11±0.40[a]	1.06±0.5[a]	0.92±0.4[b]	0.9±0.5[b]	0.77±0.1[b]	0.68±0.32[b]
7	1.23± 0.15[a]	1.23±0.20[a]	1.21±0.10[a]	1.21±0.2[a]	1.18±0.3[a]	1.16±0.21[a]	1.14±0.46[a]	1.13±0.21[a]
8	1.25±0.44[a]	1.05±0.46[a]	1.00±0.49[a]	0.92±0.5[a]	0.60±0.4[b]	0.53±0.4[b]	0.51±0.21[b]	0.47±0.21[b]
1.27±0.30[a]	1.11±0.31[a]	1.01±025[a]	0.95±0.1[a]	0.67±0.2[b]	0.53±0.12[b]	0.47±0.21[b]	0.33±0.10[b]	

Nanoparticles on the Skin of Albino Rats

Values are wound closure ± standard error of mean of triplicate determinations. Values with the same superscript in the same row and column are not significantly different from each other at ($p<0.05$).

Group 1: Diabetes +Wound + Sp + Extract, Group 2: Diabetes+Wound + Ec + Extract, Group 3: Diabetes + Wound + Kp + Extract, Group 4: Diabetes +Wound + Sa + ExtractGroup 5: Diabetes+Wound + Pa + Extract, Group 6: Diabetes+Wound + mixed organisms + Extract, Group 7: Diabetes+Wound only (-ve control), Group 8: Wound only (+ve control), Group 9: Wound + Extract.

4.1.11 Effect of extract-mediated silver nanoparticles on skin of rats

Plates V and VI revealed the histology of skin of control groups of rats and those exposed to treatment with extract mediated silver nanoparticles for 14 days. The results obtained from the study revealed that groups 1 to 6 possessed collagen, fibroblast and few inflammatory cells. Granulation tissues and blood capillaries were observed in the groups (2, 3, 4 and 5). Group 7 (negative control) possessed thinnier epithelial layer with less and loosely packed collagen, fibroblast, blood vessels and high inflammatory cells. Group 9 possessed complete epithelialization of the treated tissue with regularly arranged collagen, more fibroblast and blood vessels with few inflammatory cells.

4.1.12. The safety of the ointment

The administration of ointment on group 10 animals (control) revealed the absence of allergic skin reactions, dermitis or death.

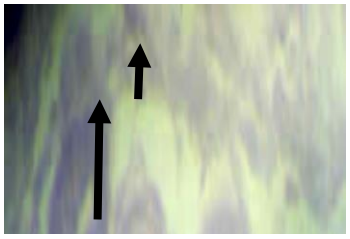

Wound + Extract Only

Complete epithelization of the Treated tissue with regularly arranged collagen, more fibro blast, blood vessels and mild

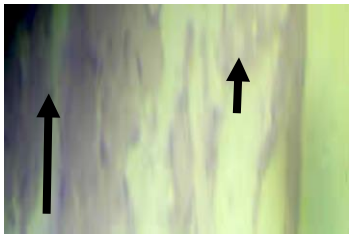

Diabetes + Wound

Thinnier epithelial layer with less and loosely packed coll agen and mild inflammatory cells.

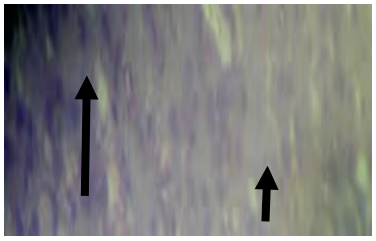

Wound Only

loosely packed collagen fibr oblast with irregular epitheli zation and mild inflammatory cells. inflammatory cells.

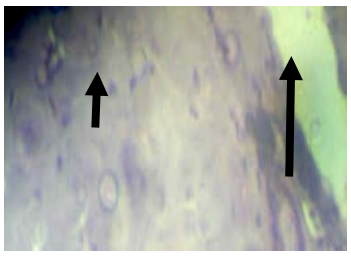

Diabetes + Wound + Sp + oint

New blood vessel formation with dense collagen deposition fibrob last and mild inflammatory cells. ory cells.

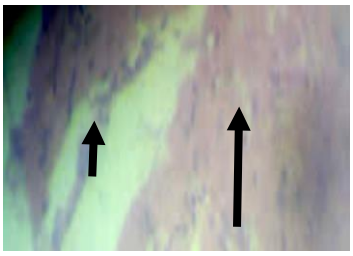

Diabetes + Wound + Kp + oint

blood vessel formation with dense collagen formation, fibroblast and mild inflammatory cells.

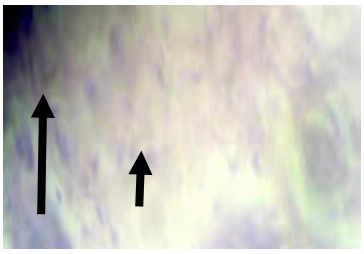

Diabetes + Wound + Sa + oint

formation of blood vessel with less dense collagen deposition, fibroblast and mild inflammat

Sp: *Streptococcus pyogenes* Kp: *Klebsiella pneumoniae* Sa: *Staphylococcus pyogenes*

Oint: ointment. Long arrow: Connective tiisue Short arrow: Fibroblast

Plate III: Effects of extract-mediated silver nanoparticles on rats' skin

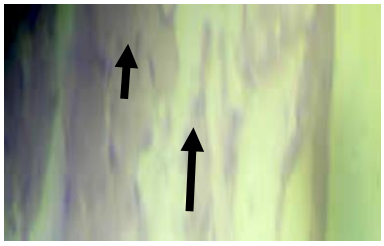

Wound + Extract only

Complete epithelization of the treated tissue with regularly arranged collagen, more fibro blood vessels with less

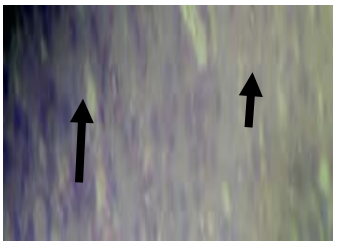

Diabetes + Wound

Thinnier epithelial layer with less and loosely packed colla gen, fibroblast, blood vessel and inflammatory vessels.

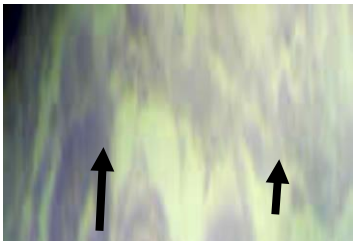

Wound only

loosely packed collagen, fibr oblast with irregular epitheli zation and mild inflammatory blast, cells. inflammatory cells.

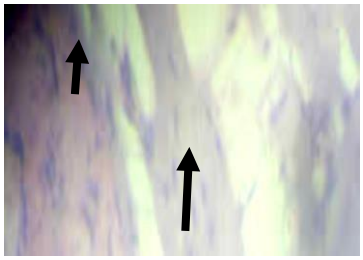

Diabetes + Wound + Ec + oint

Granulation tissue contains colla deposition, fibroblast and inflammatory cells.

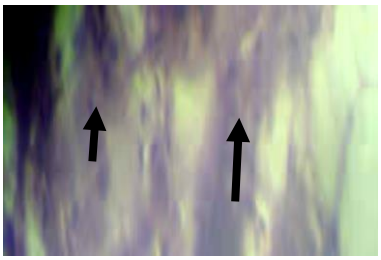

Diabetes + Wound + Pa + oint

Granulation tissue contains mild collagen, blood capillaries with less inflammatory cells.

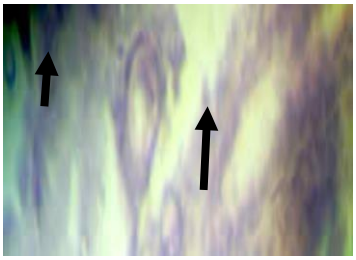

Diabetes + Wound + Mixed + oint

Gradual epithelization of tissue gen with dense collagen deposition mild fibroblast and mild inlammat ory cells.

Ec: *Escherichia coli*, Pa*: Pseudomonas aeruginosa*, Mixed: Mixed organisms

Oint: Ointment. Long arrow: Connective tiisue Short arrow: Fibroblast

Plate IV: Effects of extract-mediated silver nanoparticles on rats skin (Cont'd).

4.2 Discussion

In this study, it was observed that cyanides, phenols, flavonoids, saponins, phytates, tannins, alkaloids and oxalates were present in the crude extract of *Macrotermes bellicosus* (Table 4.2). This result corresponded with the findings of Agbaje *et al.* (2016) and Giovanna *et al*., (2020) on *M. bellicosus* possession of cyanides, flavonoids, saponins, phytates, phenols, proteins, alkaloids and tannins. Tannins and oxalates were not detected in the qualitative assessment but present in minute amount in qualitative screening of *M. bellicosus*. This may be due to experimental error and specificity and sensitivity of test reagents as defined in the experiment. In the present study, high concentration of cyanides (2247.00), saponins (321. 25), phytates (165.67), and phenols (145.21) were observed in dried powder of *M. bellicosus.* This result contradicts the report of George *et al*. (2019) in which low levels of phytates (0.421) and complete absence of phenols was observed. This may be due to differences in soil content and the feeding habits of the insects. High cyanide content is significantly toxic and poisonous to the mitochondrial electron transport chain within cells. Saponins serve as defence against diseases and herbivores (Iwalokun *et al*., 2019). Phytates has antimicrobial activity (Vikas *et al*., 2020). Phenols inactivate microbes through cell lysis and enzymes inactivation (Lyon *et al*., 2019). Alkaloids showed the inhibition of ATP-dependent transport of compounds across cell membrane (Othman *et al*., 2019). Flavonoids are known to inhibit the biofilm formation (Gorniak *et al*., 2019).

In the present study, the findings showed that many of the test isolates were coagulase negative (*Streptococcus pyogenes, Escherichia coli, Klebsiella pneumoniae and Pseudomonas aeruginosa*) and catalase positive (*K. pneumoniae, E.coli, S. aureus* and *P.aeruginosa*). They were oxidase negative (*S. pyogenes*, *S.aureus*, *E.coli* and *K. pneumoniae*) (Table 4.4). These results correspond with the findings of Abdulkader *et al*.

(2018) in which similar organisms were reported. In the study, *P. aeruginosa*, *K. pneumoniae*, *S. aureus*, *S. pyogenes* and *E. coli* were isolated from patients with diabetic foot infection. Ren *at al*. (2019) also isolated the same organisms from diabetic foot infection. Gram staining of test organisms showed Gram negative rods (*K. pneumoniae*, *P. aeruginosa* and *E.coli*) and Gram positive cocci (*S. aureus* and *S. pyogenes*). This is in line with the findings of Adelere *et al*. (2020) who used Gram staining procedure to classify similar organisms.

In this study, crude ethanol (Ee), aqueous, ethylacetate and n-hexane fractions of *M. bellicosus* were unable to inhibit the growth of *S. aureus* and *E.coli* (Table 4.1) while aqueous and ethylacetate fractions displayed low antibacterial effect against *P. aeruginosa, K. pneumoniae* and *S. pyogenes*. The inactivity of some of the extracts could be as a result of low concentration, the size of biomolecules of antibacterial compounds in the extracts, extraction capacity of the solvents and acquisition of horizontal gene transfer by *S. aureus* and *E. coli* (Abid, 2020). This result is similar with the findings of Giovanna *et al*. (2019) who screened ethanol, ethylacetate, chlorofoam and aqueous fractions of winged termites against similar test organisms used in this study. Formation of silver nanoparticles using crude extract of ethanol (Ee) and fractions (Eaq, Eoac and Eh) of *M. bellicosus* was accompanied by colour change from light-brown to dark brown. Ragaa *et al*. (2019) reported that synthesized silver nanoparticles exhibited remarkable colours changes from light-brown to dark-brown. Silver nanoparticles exhibited light yellowish colour in nhexane solution. This may be due to excitation of surface plasmon resonance (SPR) (Singh *et al*., 2017). By using UV-Visible spectrum, the maximum absorbance peak for *M. bellicosus* was observed at 410, 400, 395 and 390 nm for Eoac-AgNPs, Eh-AgNPs, EeAgNPs and

Eaq-AgNPs respectively. Similary, Sharma *et al*. (2009) reported absorption spectra of synthesized silver nanoparticles in the reaction media had absorbance peak at 420 to 450 nm.

In Figure 2, scanning electron microscopy (SEM) of synthesized silver nanoparticles was observed to be spherical and aggregated. Nanoparticles were in the size ranging from 25 to 30 nm with a variety of sizes. Mogomotsi *et al*. (2019) also observed aggregated nanoparticles in the range of 20-25 nm. Energy dispersive spectrum (EDS) of the synthesized particles was analyzed alongside SEM which exhibited signals of silver and other elements. The EDS spectrum indicated weak signals of Carbon (C), Oxygen (O),

Silicon (Si), Phosporous (P), Sulphur (S), Chlorine (Cl), Pottassium (K) and Silver (Ag). Their presence may be due to environmental interferences during sample preparation on a glass substarte (Suba *et al*., 2013). This result corresponds with the findings of Sang and Bong, (2019) who reported high presence of silver with few amount of carbon, oxygen and chlorine. Figure 3 revealed the X-ray diffraction spectrum (XRD) of silver nanoparticles as a face-centred cubic with similar diffraction profiles and numerous intense peaks at 2ɵ (9.80°, 19.85°. 30.0°, 30.0°, 35.0°, 36.8°, 40.0°, 45.0°, 49°0, 55.0°, 58.7°) which showed strong diffraction peak at 35.60°. Thus the silver nanoparticles formed were crystalline in structure (Waseda *et al*., 2011). Fourier transform infrared spectrum (FTIR) analysis confirmed that the bioreduction of Ag^{+} ions to silver nanoparticles was due to reduction by capping agents of insect extract and revealed the presence of biomolecules that include carboxylic, aldehyde, alkyl and alkyl-halides functional groups (Figure 2). Similarly, Fassioli *et al*. (2014) reported that the presence of proteins in the extract can bind to silver nanoparticles through either free amino acid or carboxyl groups in the protein. Kalishwaral *et al*. (2012) observed that silver nanoparticles obtained from the culture of *Bacillus lichenformis* had very strong inhibitory action against *S. pyogenes*, *K. pneumoniae* and *S.aureus*. The inability and low antibacterial inhibitory effect of crude extracts as compared to extractmediated silver nanoparticles could be due to the zeta potential, larger size and shape of the bioactive compounds found in crude

extracts. Pal *et al*. (2007) studied the effect of nanoparticles with spherical, rod-like and triangular shaped nanoparticles against *E. coli*. They showed that all of nanoparticles had antimicrobial activity, with the triangular nanoparticles being qualitatively more effective this agrees with the inability of the spherical shape of the extract-AgNPs used in this study to inhibit *S. aureus* and *E.coli* which also corresponds with the findings of Kim *et al*. (2007) who revealed that *S. aureus* was not inhibited by spherical AgNPs. In the present study, the antibacterial effect of Eoac-

AgNPs at 3.2 mg and amoxicillin + clavulate (0.5 µg/ml) against *P. aeruginosa* and *S. pyogenes* are not significantly ($P \geq 0.05$) different from each other. At 8 mg, the EoacAgNPs displayed higher inhibitory effect against *S. pyogenes* than the standard drug. It is likely that a combined effect between the activity of the nanoparticles and free ions contributes in different ways to produce a strong antibacterial activity of broad spectrum than the antibiotic (Amoxicillin). Combination strategies of extracts and silver nanoparticles have demonstrated strong antimicrobial properties through diverse defence mechanisms including photocatalytic production of reactive oxygen species that damage cell components and viruses, compromising the bacterial cell capsule, interruption of energy transduction and inhibition of enzyme activity and DNA synthesis.This shows that on further purification, the Eoac-AgNPs may show better inhibitory effect than what is obtainable in this study. The results of the present study revealed that extract mediated silver nanoparticles was bactericidal on the test organisms.

In this study, the injection of alloxan (150 mg/kg b.w) in all the treatment groups (1 to 6) and control groups (7 and 9) of rats confirmed the induction of diabetes as evidenced by high level of blood sugar at ≤ 270 mg/dL.

Table 4.6, showed the wound healing activity of extract ointment in rats' skin. Silver nanoparticle-formulated ointment provided emollience, even distribution of extract and anti-inflammatory effect of Vaseline and wax on the infected wounded skin. This corresponds with the findings of Arun *et al*. (2016) who made use of similar ointment preparation using *Jasminum auriculatum* vahl leaves. There was no significant wound contraction observed in all the treatment groups and control groups (7 to 9) from day 0 to day 6. The results of this study on wound healing activity revealed that the ointment formulation significantly ($P \leq 0.05$) increased wound healing effect in all the treatment groups (1 to 6) and some of the control groups 8 and 9 at day 8 as compared with control group 7 (diabetes + ointment) with no observable wound contraction.

However, the period of complete wound healing was signifcantly ($P < 0.05$) noticeable on day 14 in all the treated groups as compared with control groups 8 and 9. Demilew *et al*. (2018) reported similar findings using *Acanthus polystachyus* extract formulations on wound healing in rat models. Furthermore, Plates V and VI micrographs of animal skins revealed the possession of collagen, fibroblast and few inflammatory cells in most of the treated groups (1 to 6) as compared with control group micrographs (8 and 9). There was complete epithelialization in treated skin tissue with regularly arranged collagen, fibroblast, blood vessels and few inflammatory cells in control group 9 (Plates V & VI). The shorter period of wound area contraction and faster epithelialization could be due to the ability of ointment to enhance collagen synthesis, induction of cell proliferation (blood vessels) and antimicrobial activities of bioactive constituents in the extract-mediated silver nanoparticles. The absence of allergic reactions in group 10 animals indicated the safety of the ointment for topical application (Dons and Soosairaj, 2018).

CHAPTER FIVE

5.0 Conclusion and Recommendations

5.1 Conclusion

Pseudomonas aeruginosa, *Escherichia coli*, *Klebsiella pneumoniae*, *Staphylococcus aureus*, and *Streptococcus pyogenes* were isolated from patients with diabetic foot infection. Crude ethanol (Ee) and fractions of *M. bellicosus* contained cyanides, phenols, flavonoids, phytates, alkaloids and saponins.Very high quantities of cyanides (2247.00), saponins (321.2505), phytates (165.673), and phenols (142.2095) were detected in *M. bellicosus* powder. Crude ethanol (Ee), n-hexane (Eh), ethylacetate (Eoac), and aqueous

(Eaq) fractions of *M. bellicosus* at 200 mg/ml were inactive against *Escherichia coli* and *Staphylococcus aureus*. However ethylacetate mediated silver nanoparticles (Eoac-AgNPs) and n-hexane mediated silver nanoparticles (Eh-AgNPs) of *M. bellicosus* inhibited the growth of *P. aeruginosa*, *K.pneumoniae* and *S.pyogenes at* 200 mg/ml respectively. A dose dependent inhibitory effect was displayed by Eoac-AgNPs against *P. aeruginosa* and *S.pyogenes*. The MIC of Eoac-AgNPs of *M. bellicosus* was at 3.125 6.25 and 25.0 mm for *S.pyogenes, P. aeruginosa* and *K.pneumoniae* and *S.pyogenes.* The extract showed bactericidal effect against the test isolates.

Silver nanoparticles was synthesized using crude extracts of ethanol and portions (Ee, Eaq, Eoac and Eh) the synthesis was indicated by colour change from light brown to dark brown. The UV-Vis spectroscopy maximum absorbance was at 410, 400, 395 and 390 nm for ethylacetate, n-hexane, ethanol and aqueous extracts mediated silver nanaoparticles respectively. Fourier transform infrared (FTIR) spectrum indicated the presence of biomolecules that includes aromatic alkyl halide, carboxyl and alkynes functional groups.

Scanning electron microscopy and energy dispersive spectroscopy (SEM/EDS) of extract mediated silver nanoparticles revealed spherical morphology and aggregated nanoparticles while X-ray diffraction spectroscopy (XRD) peaks were observed at 2ɵ(10.00˚-55.65˚). The Eoac-AgNPs displayed significant ($P<0.05$) wound healing activity from day 0 to14 in diabetic rats and normal rats. Treatment of rats with ointment showed wound healing characterized by the presence of collagen, granulation tissues, few inflammatory cells and complete epitelialization. The application of Eoac-AgNPs ointment on the rats did not produce allergic reactions, dermatitis or death. Extract mediated silver nanoparticles is relatively safe for topical application in experimental animals.

5.2 Recommendations

It is recommended that:

i. Extract-mediated silver nanoparticles have a promising antibacterial action and should be considered as a combination therapy for treatment of infected wound.

ii. *Macrotermes bellicosus* mediated silver nanoparticles is topically non-toxic and should be considered as a natural source of topical antibacterial therapy for wound healing in diabetic ulcers.

iii. Further studies are recommended on structural elucidation to determine the mechanism of action of the antimicrobial compounds present in the active fractions of *Macrotermes bellicosus.*

REFERENCES

Abdulkader, M., Ayaz, A., Dania, A., Ruqaiyyah, B. S., Muhammad, R. S., & Naveed, A. K. (2018). Silver Nanoparticle Conjugation-Enhanced Antibacterial Efficacy of Clinically Approved Drugs Cephradine and Vildagliptin. *Research Institute of Chemistry*, 7(4), 100-107.

Aderibigbe, B. A. (2017). Metal-Based Nanoparticles for the Treatment of Infectious Diseases. *Molecules*, 2, 13-21.

Agbaje, L., Sunday, A. O., & Joseph, A. E. (2016). The emerging roles of arthropods and their metabolites in the green synthesis of metalic nanoparticles, 5(6): 601-622.

Aguocha, B.U., Ukpabi, J. O., Onyeonoro, U. U., Unachukwu, C. N., Uchenna, D. I., & Young E.E. (2013). Pattern of diabetic mortality in a tertiary health facility in south eastern Nigeria. *African Journal of Diabetes Medicine*, 21(4),1-3.

Ahlqvist, E., Storm, P., Käräjämäki, A., Martinell, M., Dorkhan, M., & Carlsson.A. (2018). Novel sub-groups of adult-onset diabetes and their association with outcomes: a data-driven cluster analysis of six variables. *Lancet Diabetes Endocrinology*, 6(5), 361–369.

Akkus, G., Evran, M., Gungor, D., Karakas, M., Sert, M., & Tetiker, T. (2016). "Tinea pedis and onychomycosis frequency in diabetes mellitus patients and diabetic foot ulcers. A cross sectional – observational study." *Pakistan Journal of Medical Science* 32(4), 891-895.

Albuquerque, U. P., & Rômulo, R. N. A. (2016). Introduction to Ethnobiology, Cham: *Springer*

Alves, R. R. N., Albuquerque, U. P., Raubenheimer, D., & Rothman, J. (2013). Animals as a Source of Drugs: Bioprospecting and Biodiversity Conservation. In: Alves RRN, Rosa IL, editors. Animals inTraditional Folk Medicine: *Implications for Conservation*. Heidelberg: Springer, 67–89.

Amadi, E., & Kiin-Kabari, D. (2016). Nutritional Composition and Microbiology of Some Edible Insects Commonly Eaten in Africa. Hurdles and Future Prospects: A Critical Review. *Journal of Food: Microbiology, Safety & Hygiene*, 1(1), 1-7.

Anumah, F. O., Mshelia-Reng. R., Abubakar, A., Sough, T., Asudo, F., & Jamda, M. A. (2017). Management outcome of diabetic foot ulcers in a teaching hospital in Abuja, Nigeria. *Journal of Diabetes Foot Complications*, 9(1), 15–20.

Arman, A., Parivash, D., Saeed, S., Bita, A., Habib, D., Hosein, H., & Reza, S. (2020). Frequency and Antimicrobial Susceptibility Patterns of Diabetic Foot Infection of

Patients from Bandar Abbas District, Southern Iran. *Journal of Pathogens*, 105(7), 16-27.

Arun, M., Satish, S., & Anima, P. (2016) "Evaluation of wound healing, antioxidant and antimicrobial efficacy of Jasminum auriculatum Vahl. leaves," *Avicenna Journal of Phytomedicine,* 3(6), 295-299.

Ayitso, A. S., Onyango, D. M., & Wagai. S. O. (2017).Antimicrobial Activities of Microorganisms Obtained from the gut of *Macrotermes Michaelseni* in Maseno, Kenya. *Journal of Applied Biology Biotechnology*, 3(6), 48-52.

Banerjee, P., Satapathy., & Mukhopahayay, A. (2016). Leaf extract mediated green synthesis of silver nanoparticles from widely available Indian plants: synthesis, characterization, antimicrobial property and toxicity analysis, *Bioresources and Bioprocess*, 1(1), 3-8

Ben-Shahar, Y. (2018). The impact of Environmental Mn Exposure on Insect Biology. Frontiers in Genetics, 9(10), 33-39.

Biel, M. A., Sievert, C., Usacheva, M., Teichert, M., & Balcom, J. (2016). Antimicrobial photodynamic therapy treatment of chronic recurrent sinusitis biofilms. *International Forum Allergy Rhinology*, 1(2), 329–334.

Billah, M. K., Pesewu, G. A., Hannah, O., Michael, A. O., Isaac, A. B., Nicholas, T. K., & Samuel, O. D. (2016). In Vitro antibacterial activities of cockroach extracts against selected bacterial pathogens. American Journal of Research Communication, 3(12), 78-94.

Biswas, T. K., Maity, L. N., & Mukherjee B. (2016). Wound healing potential of Pterocarpus Santalinus Linn: a pharmacological evaluation. *International journal of low extreme, Wounds*, 3(1), 143–50.

Caroll, K. C., Pfaller, M. A., Landry, M. L., McAdam, A. J., Patel, R., Richter, S. S., & Warnock, D. W. (2019). *Manual of Clinical Microbiology* and *American Society for Microbiology*, 12, 6-14.

Caroll, K. C., Pfaller, M.A., Landry, M. L., McAdam, A. J., Patel, R., Richter, S. S., & Warnock, D.W. (2019). Manual of Clinical Microbiology, 12th ed. *American Society for Microbiology.*

Centers for Disease Control and Prevention. (2017). National Diabetes Statistics Report: Estimates of Diabetes and Its Burden in the United States, Atlanta: *U.S. Department of Health and Human Services.*

Chatterjee, S. S., Joo, H. S., Duong, A.C., Dieringer, T. D., Tan, V.Y., Song, Y., Fischer, E. R., Cheung, G. Y., Li, M., & Otto, M. (2016). Essential *Staphylococcus aureus* toxin export system. *Natural Medicine,* 19, 364–367.

Chaves, T. P, Clementino, E .L. C., Felismino, D. C., Alves, R. R. N., Vasconcellos, A., & Coutinho, H. D. M. (2014). Antibiotic resistance modulation by natural products obtained from Nasutitermes corniger (Motschulsky, 1855) and its nest. S*audi journal Biological Science*. In press.

Dehghanizade, S., Arasteh, J., & Mirzaie, A. (2018). Green synthesis of silver nanoparticles using Anthemis atropatana extract: Characterization and in vitro biological activities. *Artificial Cell Nanomedicine Biotechnology*, 46(5), 160-168.

Demilew, W., Mequanint, G. A., & Asrade, S. (2018). Evaluation of the Wound Healing Activity of the Crude Extract of Leaves of Acanthus polystachyus Delile (Acanthaceae). *Evidence-Based Complementary and Alternative Medicine*, 9.

DeSantis, C. E., Siegel, R. L., Sauer, A. G., Miller, K. D., Fedewa, S. A., Alcaraz, K. I., & Jemal, A. (2016). Cancer statistics for African-Americans, Progress and opportunities in reducing racial disparities. *CA Cancer Journal of Clinicals*, 66-67.

Dobermann, D., Swift, J.A., & Field, L.M. (2017). Opportunities and hurdles of edible insects for food and feed. Nutrition Bulletin, 42(4), 293-308.

Dons, T., & Soosairaj, S. (2018). Evaluation of Wound Healing Effect of Herbal Lotion in Albino Rats and its Antibacterial Activities. *Clinical Phytoscience*, 4(6), 123-127.

Döring, G., Bragonzi, A., Paroni, M., Akturk, F. F., Cigana, C., Schmidt, A., & Ulrich, M. (2016). BIIL 284 reduces neutrophil numbers but increases *P. aeruginosa* bacteremia and inflammation in mouse lungs. *Journal of Cystic Fibrosis,* 13(2), 156-163.

Dos Santos, C. A., Seckler, M. M., Ingle, A. P., Gupta, I., Galdiero, S., Galdiero, M., Gade, A., & Rai, M. (2017). Silver nanoparticles: Therapeutical uses, toxicity, and safety issues. *Journal of Pharmaceutical Science,* 103(9), 1931–1944.

Endo, H., Kase, S., and Takahashi, M. (2020). “Relationship between diabetic macular edema and choroidal layer thickness, 15(1), 12-22.

Figueirêdo, C. R, Rozzanna, E., Alexandre, V., Iamara, S. P., & Rômulo, R. N. A. (2016). Edible and medicinal termites: a global overview. *Journal of Ethnobiology and Ethnomedicine,* 11, 29-35.

Franchi, L., Muñoz-Planillo, R., and Núñez, G. (2017). Sensing and reacting to microbes through the inflammasomes. *Natural Immunology*, 13(3), 325-332.

Garcia-Sureda, L., Domenech-Sanchez, A., Barbier, M., Juan, C., Gasco, J., & Alberti, S. (2016). OmpK26, a novel porin associated with carbapenem resistance in *Klebsiella pneumoniae*. *Antimicrobial Agents Chemotherapy*, 55(10), 4742–4747.

Geethalakshmi, R., & Sarada, D. V. L. (2016). Gold and silver nanoparticles from Trianthema decandra: synthesis, characterization, and antimicrobial properties. *International Journal of Nanomedicine*, 7(11), 5375–5384.

George, B.P.A., Kumar, N., Abrahamse, H., & Suprakas, S.R. (2019). Apoptotic efficacy of multi-faceted biosynthesized silver nanoparticles on human adenocarcinoma cells. *Scientific Report*, 8(1), 1-14.

Giovanna, M., Marisa, M.B., Adriano, F.F., Carlos, A.F., Ricardo, R.B.C., and Sergio, R.T. (2020). Silver nanoparticles obtained in PAH/PAA-Based Multilayers by Photochemical Reaction. *Journal of Physics and Chemistry*, 113(14), 19005-19010.

Gorniak, I., Bartoszewski, R., & Kroliczewski, J. (2019). Comprehensive review of antimicrobial activity of plant flavonoids. *Phytochemical Review*, 18(1), 241-272.

Gupta, A., Eral, H. B., & Hatton, T. A. (2016). Nanoemulsions: Formation, properties and applications. *Soft Matter*, 12(4), 2826-2841.

Hamsa, I.A., Hind, A. A., & Hayam, S.A. (2019). Green Synthesis of Silver Nanoparticles using Cinnamomum Zylinicum and their Synergistic Effect against Multi-Drug Resistance Bacteria. *Journal of Nanotechnology Research*, 1(3), 095-107.

Handayani, D., & Amina, I. (2017). Antibacterial and cytotoxic activities of ethylacetate extract of symbiotic fungi from west Sumatra marine sponge. *Acanthromgylophora ingens*, *Journal of Applied Pharmaceutical Science*, 7(2), 237-240.

Hatipoglu, M., Mutluoglu, M., Turhan, V., Uzun, G., Lipsky, B. A., Sevim, E., Demiraslan, H., Eryilmaz, E., & Ozuguz, C. (2016). Causative pathogens and antibiotic resistance in diabetic foot infections: A prospective multi-center study. *Journal of Diabetes Complications*, 30(7), 910–916.

Hoffmann, M., Kujath, P., Flemming, A. M., Begum, N., and Zimmermann, M. (2016). Survival of diabetes patients with major amputation is comparable to malignant disease. *Diabetic Vascular Diseases Research*, 12(5), 265–71.

Institute for Laboratory Animal Research Council (2011). Guide for the care and use of Laboratory Animal 8th edition. National Academies Press, Washinton DC US, 5660.

Iwalokun, B. A., Akinloye, O., Udoh, B. E., & Akinyemi, K. O. (2019). Efficacy of silver nanoparticles against multi-drug resistant clinical Staphylococcus aureus isolates from Nigeria. *Journal of Immunoassay and Immunochemistry*, 40(2), 214-236.

Jadhav, K., Dhamecha, D., & Bhattacharya, D. (2016). Green and ecofriendly synthesis of silver nanoparticles: Characterization, biocompatibility studies and gel formulation for treatment of infections in burns. Journal of Photochememistry, *Photobiology and Bioliology*, 155(16), 109-115.

Jilie, K., & Shaoning. (2017). Fourier Transform Infrared spectroscopic analysis of protein secondary structures, *Acta Biochemistry and Biophysics Science* 39(8), 549-559.

Jneid, J., Cassir, N., Schuldiner, S., Jourdan, N., Sotto, A., Lavigne, J. P., & La, S. B. (2018). Exploring the microbiota of diabetic foot infections with culturomics. *Front Cellular Infection Microbiology*, 8(4), 282-287.

Jongema, W. (2017). List of edible insect species of the world. *Waganingen, Laboratory of Entomolgy*. Retrieved from, www.ent.wur.nl/UK/Edible+insects/Worldwide+ species+list.

Jouquet, P., Blanchart, E., & Capowiez, Y. (2014). Utilization of Earthworms and Termites for the restoration of the Ecosystem functioning. *Applied Soil Ecology*. 73(1), 3440.

Kalishwaralal, K., BarathManiKanth, S., Pandian, S. R., Deepak, V., & Gurunathan, S. (2016). Silver nanoparticles impede the biofilm formation by *Pseudomonas aeruginosa* and Staphylococcus epidermidis. *Colloids Surface Biointerfaces*, 79 (5), 340–344.

Kelkawi, A.H.A., Abbasi, Kajani, A., & Bordbar, A.K. (2017). Green synthesis of silver nanoparticles using Menthapulegium and investigation of their antibacterial, antifungal and anticancer activity. *IET Nanobiotechnology*, 11(4), 370-376.

Kim, J. S., Kuk, E., Yu, K. N., Kim, J. H., Park, S. J., Lee, H. J., Kim, S. H., Park, Y. K., Park, Y. H. & Hwang, C. Y. (2007). *Antimicrobial effects of silver nanoparticles*, *Nanomedicine*, 3(2), 95–101.

Kinyuru, J. N., Konyole, S. O., Roos, N., Onyango, C. A., Owino, V. O., & Owiuor, B. B. (2016). Nutrient composition of four species of winged termites consumed in western Kenya. *Journal of Food Composition Analysis*, 30 (7), 1–19.

Latunde-Dada, G.O, Yang, W., & Aviles, M.V. (2016). In vitro iron availability from insects and sirloin beef. *Journal of Agricultural and Food Chemistry*, 64(44), 84208424.

Lavery, A., Armstrong, D. G., Quebedeaux, T., & Fleishli, J. G. (2017). Practical criteria for screening patients at high risk for diabetic foot ulceration. *Archived international medicine*, 158(5), 157-162.

Lavigne, J. P., Sotto, A., Dunyach-Remmy, C., & Lipsky, B. A. (2017). New molecular techniques to study the skin microbiota of diabetic foot ulcers. *Advanced Wound Care*, 13(4), 209-213.

Leslie, R. D., Palmer, J., Schloot. N. C., & Lernmark, A. (2016). Diabetes at the crossroads: relevance of disease classification to pathophysiology and treatment. *Diabetologia*, 59(1), 13–20.

Lijun Y., Yang, G., Jinjian, L., Yumin, Z., Chunhua, R., Jing, W., Zhongqiang, W., Jianfeng, L., Liping, C., Wei, W., & Fan, H. (2018). Silver-Coated Nanoparticles Combined with Doxorubicin for Enhanced Anticancer Therapy. *Journal of Biomedical Nanotechnology*, 14(5), 312-320.

Lipsky, B. A. Aragon-Sanchez, J., Embil, J., Kono, S., Lavery, L., Senneville, E., UrbancicRovan, V., Van Asten, S., & Peters, E. J. G. (2016). International Working Group on the Diabetic Foot (IWGDF). IWGDF guidance on the diagnosis and management of foot infections in persons with diabetes. *Diabetes Metabolite Research Revison*, 32(3), 45–74.

Liu, X., Liang, J., Jiang, Y., Wang, B., Yuan, H., Zhang, L., Zhou, Y., Xu, H., & Zhou, W. (2016). Molecular characteristics of community-acquired methicillin-resistant *Staphylococcus aureus* strains isolated from outpatients with skin and soft tissue infections in Wuhan, China. *Pathogenic Disease*, 74(2), 654-659.

Manikandan, V., Velmurugan, P., & Park, J.H, (2017). Green synthesis of silver oxide nanoparticles and its antibacterial activity against dental pathogens. *Journal of Biotechnology*, 7(3): 72-83.

Masson, F., Vallier, A., Vigneron, A., Balmand, S., Vincent-Monegat, C., & ZaidmanRemy, A. (2016). Systemic infection generates a local-likeimmuneresponseof the bacteriomeorganin insectsymbiosis. *Journal of Innate Immunology*, 7(3), 290–301.

Meyer-Rochow, V. B., & Chakravorty, J. (2016). Notes on entomophagy and entomotherapy generally, and information on the situation in India inparticular, *Applied Entomology Zoology*, 48(3), 105–12.

Min, L., Wei, Z., Zhaoli, Y., & Xiangzhen, Y. (2018). Smoking increases the risk of diabetic foot amputation: A meta-analysis. *Experimental and Therapeutic Medicine*, 15(2), 1680–1685.

Miyan, Z., Fawwad, A., Sabir, R., & Basit, A. (2017). Microbiological pattern of diabetic foot infections at a tertiary care center in a developing country. *Age Years*, 53 (2), 10–20.

Mogomotsi, K., Oluwole, S., Aremu, A., & Ramokone, G. (2019). Characterization and Antibacterial Activity of Biosynthesized Silver Nanoparticles Using the Ethanolic Extract of Pelargonium sidoides DC. *Journal of Nanomaterials*, 10(1), 11-15.

Muhammad, A.R., Zakia, K., Saira, R., & Shahzad, N. (2016). Synthesis, characterization and antibacterial properties of nano-sized cobalt particles. *Advances in Civil, Environmental, and Material Research*, 1(1), 3-9.

Narayan, K. M., & Kelly, W. (2016). Type 2 diabetes: Why we are winning the battle but losing the war. Award Lecture. *Diabetes Care*, 39(5), 653–663.

Nada, S.E., Williams, F.E., & Shah, Z.A. (2017). Development of a Novel and Robust Pharmacological Model of Okadaic Acid-Induced Alzheimer's disease in Zebrafish. CNS & Neurological disorders drug targets. *The Zebrafish Information Network*, 15(1), 86-94.

Narayan, K. M., Pasquel, F. J., Umpierrez, G. E., Fuchsberger, C., & Flannick, J. (2016). Type 2 diabetes: Why we are winning the battle but losing the war. 2015 Kelly West Award Lecture. *Diabetes Care*, 39(3), 653–663.

Ng, L. Y., Akil, A., & Abdul W. M. (2017). Synthesis and Characterization of Silver Oxide Nanoparticles by a Novel Method.*International Journal of Scientific and Engineering Research*, 4.

Nicoli, S., Padula, C., Aversa, V., Vietti, B., Wertz, P. W., Millet, A., Falson, F., Govoni. P. & Santi P. (2018). Characterization of Rabbit ear skin as a skin model for in vitro transdermal permeation experiments: histology, lipid composition and permeability. *Skin Pharmacology Physiology*, 21(6), 218-226.

Odusan, O., Amoran, O.E., & Salami, O. (2017). Prevalence and pattern of Diabetic Foot Ulcers among adults with Diabetes mellitus in a secondary health care facility in Lagos, Nigeria. *Annuals of Health Research*, 3(2), 98–104.

Oibiokpa, F., Akanya, H., Jigam, A., & Saidu, M. (2017). Nutrient and Antinutrient Compositions of Some Edible Insect Species in Nothern Nigeria. *Journal of Natural and Applied Sciences*, 6(1), 9-24.

Okoli, S., & Iroegbu, C. U. (2005). In Vitro Antibacterial Activity of Synclisa scabrida whole Root Extracts. Academic Journals, 4(9), 946-952.

Omar, A., Wright, J. B., Schultz, G., Burrell, R., & Nadworny, P. (2017). Microbial biofilms and chronic wounds, *Microorganisms,* 5(1), 9.

Othman, L., Sleiman, A. and Abdel-Massih, R. M. (2019). Antimicrobial activity of Polyphenols and Alkaloids in the Middle Eastern Plants. *Front Microbiology*, 10 (2), 911-916.

Otto, M., Valeva, A.., Walev, I., Pinkernell, M., Sotto, A., Richard, J.L., Messad, N., & Molinari, N. (2018). *Staphylococcus aureus* toxins. *Curriculum Opinion Microbiology*, 17(1), 32–37.

Padilla, E., Llobet, E., Domenech-Sanchez, A., Martinez-Martinez, L., Bengoechea, J. A., & Alberti, S. (2016). *Klebsiella pneumoniae* AcrAB efflux pump contributes to antimicrobial resistance and virulence. *Antimicrobial Agents Chemotherapy*, 54(1), 177–183.

Pal, S., Tak, Y. K., & Song, J. M. (2017).Does the antibacterial activity of silver nanoparticles depend on the shape of the nanoparticle? A study of the Gramnegative bacterium *Escherichia coli*. *Applied Environmental Microbiology*, 73(6), 1712– 1720.

Parravano, M., De Geronimo, D., and Scarinci, F. (2019). "Progression of diabetic microaneurysms according to the internal reflectiv- ity on structural optical coherence tomography and visibility on optical coherence tomography angiography," *American Journal of Ophthalmology*, 198(7), 8–16.

Pérez-Herrero, E., & Fernández-Medarde, A. (2017). Advanced targeted therapies in cancer: Drug - nanocarriers, the future of chemotherapy. *Europe Journal of Pharmacy and Biopharmarcy*, 93(2), 52-58.

Periasamy, S., Joo, H. S., Duong, A. C., Bach, T. H., Tan, V. Y., Chatterjee, S. S., Cheung, G. Y., & Otto, M. (2017). How *Staphylococcus aureus* biofilms develop their characteristic structure, *National Academic Sciience, USA*, 109(12), 1281–1286.

Rada, B., Gardina, P., Myers, T. G., & Leto, T. L. (2016). Reactive oxygen species mediate inflammatory cytokine release and egfr-dependent mucin secretion in airway epithelial cells exposed to *pseudomonas aeruginosa*, *Mucosal immunology, 4*(2), 158-171.

Ragga, A. H., Mervat, H.H., & Salwa, S. B. (2019). Synthesis and biological characterization of silver nanoparticles derived from the Cyanobacterium Oscillatoria limnetica. *Scientific Report*, 9(1), 13071-13074.

Raghav, A., Khan, Z. A., Labala, R. K,. Ahmad, J., Noor, S., and Mishra, B. K. (2018). "Financial burden of diabetic foot ulcers to world: A progressive topic to discuss always," *Therapeutic Advances in Endocrinology and Metabolism*, 9(1), 29–31.

Rai, M., Deshmukh, S. D., Ingle, A. P., Gupta, I. R., Galdiero, M., & Galdiero, S. (2016). Metal nanoparticles: The protective nanoshield against virus infection. *Critical Review Microbiology*, 1–11.

Rai, V. R., & Bai, A. J. (2017). Nanoparticles and their potential application as antimicrobials. In: Méndez-Vilas A. ed. Science against microbial pathogens: *Communicating current research and technological advances*, 1(3), 197-209.

Raimi, T. H., & Fasanmade, O. A. (2018). Precipitating Factors for Diabetes Foot Ulcer in a Nigerian Tertiary Hospital. *European Journal of Biology and Medical Science Research*, 6(2), 21-28.

Rajakumar, G., Gomathi, T., & Thiruvengadam, M. (2017). Evaluation of anticholinesterase, antibacterial and cytotoxic activities of green synthesized silver nanoparticles using from Millettia pinnata flower extract. *Journal of Microbiology Pathogens*, 103(53), 123-128.

Regueiro, V., Moranta, D., Frank, C. G., Lawlor, M. S., Handley, S. A., Miller, V. L., Campos, M. A., Pons, J., Alberti, S., & Bengoechea, J. A. (2018). *Klebsiella pneumoniae* subverts the activation of inflammatory responses in a NOD1dependent manner. *Cellular Microbiology*, 13(1), 135–153.

Rejinold, N. S., Thomas, R. J., Muthiah, M., Lee, H. J., Jeong, Y. Y., Park, I., & Jayakumar, R. (2016) Breast tumor targetable Fe3O4 embedded thermo-responsive nanoparticles for radiofrequency assisted drug delivery. *Journal of Biomedical Nanotechnology*, 12(2), 43-48.

Ren, Y. K., Ruben, J. K., Zaharul, A. M., & Edsimo, K. (2019). Microbiology of diabetic foot infections in three district hospital in Malaysia and comparison with South East Asian Countries. *The Medical Journal of Malaysia*, 74(5), 394-399.

Richard, J. L., Sotto, A., & Lavigne, J. P. (2017). New insights in diabetic foot infection.*World Journal of Diabetes*, 2 (1), 24-32.

Riggi, L., Veronesi, M., Verspoor, R., MacFarlane, C., & Tchibozo, S. (2017). Exploring entomophagy in Northern Benin: Practices, perceptions and possibilities. *Book of Abstracts of Conference on Insects to Feed the World*.

Riggi, L.G., Veronesi, M., Goergen, G., Macfarlane, C., & Verspoor, R.L. (2016): Observations of entomophagy across Benin-Practices and Potentials. *Food Security*, 8(2), 139-149.

Roy, R., Saurabh, K., Shah, D., Chowdhury, M., and Goel, S. (2019). "Choroidal hyperreflective foci: a novel spectral domain opti- cal coherence tomography biomarker in eyes with diabetic macular edema," Asia-Pacific *Journal of Ophthalmology*, 8(4), 314–318.

Sabir, A., Ohwovoriole, A., & Isezuo, S. (2016). Type 2 diabetes mellitus and its risk factors among the rural Fulanis of Northern Nigeria. *Annual African Medicine*, 12(3), 217-222.

Sadriwala, Q., Gedam, B., & Akhtar, M. (2018). Risk factors of amputation in diabetic foot infections. *International Surgery Journal*, 5(3), 1399–1402.

Samiksha, P. D., & Dayanand P. G. (2016). Wound Healing Activity of AntiHaemorrhoidal Ointment on Rats. *Human Journals*, 5(3), 95-107.

Sang, H. L., & Bong, H. J. (2019): Silver nanoparticles: Synthesis and Application for Nanomedicine. *International Journal of Molecular Sciences*, 20(4), 865-869.

Serra, R., Grande, R., Butrico, L., Rossi, A., Settimio, U. F., Caroleo, B., Amato, B., Gallelli, L., & De Franciscis, S. (2017). Chronic wound infections: The role of *Pseudomonas aeruginosa* and *Staphylococcus aureus*. Expert Rev. *Anti-Infection Therapy*, 13(2), 605–613.

Sharma, V. K., Yngard, R. A., and Lin, Y. (2017). Green synthesis and their antimicrobial activities. *Journal of Colloid and Interface*, 145(2), 83-96.

Shockley, M., Dossey, A. T., Van-Huis, H., Johnson, D. V., Van-Huis, H., & Wilsanand V. (2017). Insects for Human Consumption. In: Morales-Ramos J, Rojas G, ShapiroIlan DI, editors. *Mass Production of Beneficial Organisms*. *London: Elsevier*, 617– 52.

Siddiqi, K.S., Husen, A., & Rao ,R.A.K. (2018). A review on biosynthesis of silver nanoparticles and their biocidal properties. *Journal of Nanobiotechnology*, 16(11), 14-19.

Singh, N., Armstrong, D. J., & Lipsky, B. A. (2016). Preventing Foot Ulcers in Patients with Diabetes. *JAMA*, 293(7), 127–218.

Skyler, J. S., Bakris, G. L., Bonifacio, E., Darsow, T., Eckel, R. H., & Groop, L. (2017). Differentiation of diabetes by pathophysiology, natural history, and prognosis. *Diabetes*, 66 (3), 241–255.

Spichler, A., Hurwitz, B. L., Armstrong, D. G., & Lipsky, B. A. (2017). Microbiology of diabetic foot infections: from Louis Pasteur to 'crime scene investigation'. *BMC Medicine*, 13(1), 2-7.

Suciu, C.O., Vlad, I.S., & Simona, D.N. (2020). Optical Coherence Tomography (Angiography) Biomarkers in the Assessment and Monitoring of Diabetic Macular Edema. *Journal of Diabetes Research,* 11(5), 55-65.

Sumatra, F. T., Paul, W. G., Agus, S., David, O. G. (2017). Meidcinal Plants from Riau Pronvince, Sumatra, Indonesia. Part2: Antibacterial and Antifungal Activity. *Journal of Ethnopharmacology*, 45(2), 97-111.

Sweet, M. J., Chesser, A., & Singleton, I. (2017). Review: Metal-based nanoparticles; size, function, and areas for advancement in applied microbiology. *Advanced Applied Microbiology*, 80(1), 113–142.

Teow, S. Y., Wong, M., & Yap, H. Y. (2018). Bactericidal Properties of Plants-Derived Metal and Metal Oxide Nanoparticles (NPs). *Molecules*, 23, 1366.

Toru, M., Junichi, T., Tomoyuki. N., & Naoya, S. (2016). Antibiotics production by an actinomycete isolated from the termite gut. *Journal of Basic Microbiology*, 52(1), 731-735.

Trzybinski, D., Niedzialkowski, P., Ossowski, T., Trynda, A., & Sikorski, A. (2016). Single-Crystal X-ray Diffraction Analysis of Designer Drugs: Hydrochlorides of Metaphedrone and Pentedrone. *Forensic Science International*, 232(5),1–3, 28–32.

Van Huis, A. (2017). Cultural Significance of termites in sub-Saharan Africa. *Journal of Ethnobiology and Ethnomedicine,* 13(4), 1-12.

Vandenesch, F., Lina, G., & Henry, T. (2016). *Staphylococcus aureus* hemolysins, bicomponent leukocidins, and cytolytic peptides: A redundant arsenal of membranedamaging virulence factors? Front. *Cellular Infection Microbiology*, 2(1), 12-16.

Velusamy, P., Kumar, G. V., & Jeyanthi, V. (2016). Bio-inspired green nanoparticles: Synthesis, mechanism, and antibacterial application. *Toxicology Research*, 32(11), 95–102.

Verma, A. K., & Prasad, S.B. (2016). Antitumor effect of blister beetles: an ethnomedicinal practice in Karbi community and its experimental evaluation against a murine malignant tumor model. *Journal of Ethnopharmacology*, 148(3), 869–879.

Wang, L., Hu, C., & Shao, L. (2017). The antimicrobial activity of nanoparticles: present situation and prospects for the future. *International Journal of Nanomedicine*, 12(31), 1227-1249.

Wei, Q., & Ma, L. Z. (2016). Biofilm matrix and its regulation in *Pseudomonas aeruginosa*. *International journal of molecular sciences*, *14*(10), 20983-21005.

Wolcott, R. D., Rumbaugh, K. P., & James, G. (2017). Biofilm maturity studies indicate sharp debridement opens a time- dependent therapeutic window. *Journal of Wound Care*, 19(3), 320-328.

Woodmansey, C., McGovern, A. P., McCullough, K. A., Whyte, M. B., Munro, N. M., & Correa, A. C. (2017). Incidence, demographics, and clinical characteristics of diabetes of the exocrine pancreas (Type 3c): a retrospective cohort study. *Diabetes Care*. 40(6), 1486–1493.

World Health Organization (2019). Definition, diagnosis and classification of diabetes mellitus and its complications. Part 1.

World Health Organization Guideline. (2020). Diagnostic criteria and classification of hyperglycaemia first detected in pregnancy: *Diabetes Research Clinical Practical*, 103(9), 341–363.

Wu, X., Ren, F., Qiu, C., & Wu, H. (2017). Successive extracting saponins and polysaccharides from lily, *Journal of Chromatography*, 1218(8), 5765-5773.

Xu, Y., Rong, A., Xu, W., Niu, Y., & Wang, Z. (2017). "Comparison of 12-month therapeutic effect of conbercept and ranibizumab for diabetic macular edema: a reallife clinical practice study," *BMC Ophthalmology*, 17(1), 158-167.

Yi, H. Y., Chowdhury, M., Huang, Y. D., & Yu, X. Q. (2017). Insect antimicrobial peptides and their applications. *Applied Microbiology Biotechnology*, 98(13), 58075822.

Zenelaj, B., Bouvet, C., Lipsky, B. A., & Uckay, I. (2016). Do diabetic foot infections with methicillin-resistant *staphylococcus aureus* differ from those with other pathogens? *International Journal of Low Extreme Wounds*, 13(4), 263-272.

Zeng Y., Hu, X.P., & Suh, S.J. (2016). Characterizationof AntibacterialActivitiesof Eastern Subterranean Termite, *Reticulitermes flavipes* against Human Pathogens. *Journal Pone*, 11(9), 13-17.

Zia, M., Gul, S., & Akhtar, J. (2017). Green synthesis of silver nanoparticles from grape and tomato juices and evaluation of biological activities. *IET Nanobiotechnology*, 11 (2), 193-199.

APPENDIX 1

Image of Termitarium

APPENDIX 2

Antimicrobial activity of n-hexane against *Pseudomonas aeruginosa* and *Escherichia coli*